J. Fluid Mech. (1965), *vol.* 22, *part* 4, *pp.* 625–656
Printed in Great Britain

Flow in the wake of self-propelled bodies and related sources of turbulence

By EDUARD NAUDASCHER
Institute of Hydraulic Research, University of Iowa

(Received 27 January 1965)

In the steady-state counterpart of the wake behind a totally immersed, self-propelled body, simulated in an air tunnel by a concentric nozzle and disk, measurements were made of mean-flow velocity and pressure, turbulence intensities in the three co-ordinate directions, turbulent shear, and mean temporal gradient and auto-correlation of the axial-velocity fluctuations. Through the equations of momentum and energy for the mean and the turbulent motion, the experimental data were used to verify the condition of self-propulsion and the accuracy of measurement, and to provide a picture of the force field and the process of energy transformation.

The variation of the principal flow characteristics was analysed with the aid of appropriate hypotheses as to the transport mechanism and the structure of the turbulence. Two hypotheses proved to be most useful: a more general concept of self-preservation than is known from elementary free-turbulence flows; and the assumption that beyond an intial shear zone the turbulence can be regarded as having originated at a point source in the flow. Extension of the analysis to flows past line and plane sources of turbulence then permitted its validity to be tested with the extensive experimental information available on decaying homogeneous turbulence behind a grid. The rates of diffusion and decay were first deduced in terms of the conventional power laws and thereafter, on the assumption of proportionality of all length scales for any one flow, in terms of more elaborate relationships. The most noteworthy results of the latter approach are the asymptotic development of wake widths and eddy scales toward constant values and the elimination of the subdivision of the flow field into a number of decay zones of vaguely defined limits that has been customary in the theory of homogeneous turbulence. Agreement with corresponding experimental results for a self-propelled body and a grid (i.e. for a point and a plane source of turbulence) was obtained over the entire available ranges of measurement.

1. Introduction

Experimental information on various elementary types of free-turbulence shear flows, mainly on jets and wakes, has become almost as comprehensive in recent years as that on homogeneous turbulence. Advances have also been made with respect to the analytical prediction of the distribution and the development of mean-flow and turbulence characteristics. Moreover, refined investigations of the turbulent structure have furthered our understanding of the turbulent-flow

processes and helped at least to disclose, if not eliminate, many inadequacies of the available theories. In all these advances engineers had an active part because of the relevance of a great number of engineering problems; nevertheless, one type of free-turbulence flow with widespread practical application—flow in the wake of a body with hydrodynamic self-propulsion—has received almost no attention to date.

In order to provide experimental information about the wake flow behind a completely immersed, axisymmetric, self-propelled body travelling at constant speed, the steady-state equivalent of this flow was simulated in an air tunnel through the principle of relative motion and studied under two aspects: first, as a process of production, convection, diffusion, and dissipation of turbulence; secondly, as a continuous and systematic change of mean-flow and turbulence patterns and their respective characteristics. Measurements of root-mean-squares, mean cross-products, and auto-correlations of the turbulent velocity fluctuations, as well as mean velocity and mean pressure, were evaluated with the aid of the pertinent equations of motion in order to check the consistency of measurements, to bring out the interrelation and understand the significance of the two aspects of the flow process, and to provide means of prediction wherever possible.

It is the essential lack of disturbance of the mean flow which distinguishes the wake of a self-propelled body from ordinary wakes and makes it an interesting subject for systematic investigation. While a towed body represents the external application of a force which strains the flow as it produces turbulence energy, a body which is self-propelled represents an essentially direct and strainless input of turbulence energy. In consequence, the flow behind a self-propelled body should be expected to have only such overall properties in common with ordinary wake flow as inhomogeneity and intermittency, but to be characterized otherwise by shear-free energy transformation like homogeneous turbulence behind a grid. As a matter of fact, the mechanisms by which turbulence energy is produced by a self-propelled body and a grid reveal a remarkable similarity. Except in an initial region strained by locally counteracting forces—drag and propulsive force near the body, drag and pressure drop near the grid—the first can be considered a point source of turbulence to the same degree of approximation as the second simulates a plane source. A coherent analysis of the flows past a point, a line, and a plane source of turbulence as axisymmetric, two-dimensional and one-dimensional counterparts is thus in order. Not only should the generality of the analysis thereby be increased, but more experimental material should become available to test its validity, and a new basis should be gained for a critical re-examination of the customary assumptions in the theory of homogeneous turbulence.

2. Experimental equipment and technique

Experiments were performed in an air tunnel with a 5 ft. wide, octagonal test section of the Iowa Institute of Hydraulic Research, at a velocity of 60 ft./sec. The self-propelled body was simulated by a stationary disk of 1·8 in. diameter

mounted on the end of a tube of 0·437 in. inner diameter at the tunnel axis, 1·5 ft. past the bell-mouth entrance of the test section (see figure 1). Flow was provided through the pipe to yield a jet with just sufficient thrust to reduce to zero the net force on the pipe-disk arrangement. The air for the jet was supplied from the 12 × 12 ft. plenum chamber of the air tunnel by a blower, and was passed through a cooling system in order to compensate for the temperature increase in the blower. The disk was held in place by four spring-steel wires of 0·008 in. diameter. The wake effect of these wires as well as the wall effect of the tunnel was found to be negligible (Ridjanovic 1963).

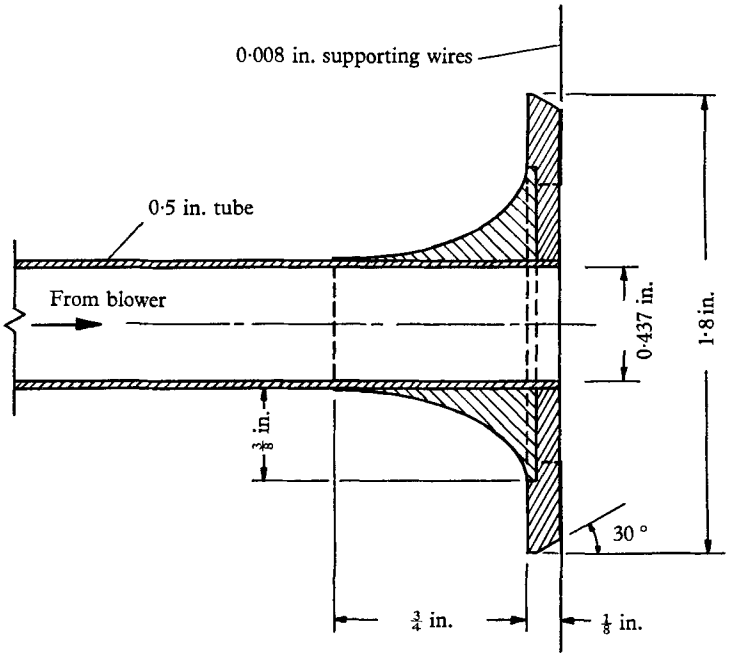

FIGURE 1. Details of test apparatus.

Preliminary tests were conducted to produce a free stream with a deviation from a uniform velocity distribution of less than 0·1 %, with a turbulence level of less than 0·2 %, and with a negligible longitudinal pressure variation. Great pains were taken to establish axial symmetry of the flow past the disk. It was found that, even with the boundary-layer separation upstream from the disk controlled by the transition piece shown in figure 1, the symmetry was very markedly affected by the slightest change in alignment of pipe and disk. With axial symmetry finally realized, the variation of flow characteristics was determined by only one measurement traverse in each cross-section.

The static pressure at a point was measured with a hypodermic-needle static tube of 0·049 in. diameter. The mean velocity was obtained from the difference between the readings of the static tube and a blunt-ended stagnation tube with an outer and inner diameter of 0·042 and 0·025 in. Both the static and the stagnation tube could be mounted interchangeably on a horizontal traversing mechanism indicating the radial position to 0·001 ft. and connected to a differ-

ential micromanometer reading to 0·001 in. of alcohol. Where necessary, the precision of measurement was increased fourfold by tilting the manometer. The readings were taken with reference to a known static pressure and stagnation pressure, respectively, within the flow. A more detailed description of the instruments and the corrections applied for their use in turbulent flow is given by Ridjanovic (1963) and Wang (1965).

For the measurement of the turbulence characteristics $\overline{u'^2}$, $\overline{v'^2}$, $\overline{w'^2}$, $\overline{u'v'}$, $\overline{(\partial u'/\partial t)^2}$, and R_τ, a IIHR hot-wire anemometer, type T-A, and a IIHR mean-square analyser, type QK 329, were used, the first of which operates on the principle of constant temperature as described by Hubbard (1957). The sensing elements of the single- and crossed-wire probes were made of a 0·00012 in. platinum-coated tungsten wire with a copper plating that was etched to give the wire a cold resistance of 4–5 Ohms. The distance between the crossed wires was kept near 0·025 in. The effect of the unavoidable asymmetry in the crossed-wire probe was eliminated by taking double sets of readings, rotating the instrument 180° about the axis of flow direction between sets. On the assumption that the energies of two uncorrelated turbulent fields superpose linearly, the measured squared intensities were corrected by subtracting the respective squares of the local air-tunnel turbulence intensities.† In regions far downstream from the turbulence source and along the edges of the diffusion zone, this correction was quite substantial.

The significant scales of the turbulence and the energy distribution among them were determined from measurements of the auto-correlation and the one-dimensional power spectrum. The auto-correlation function of the axial-velocity fluctuation

$$R_\tau = \overline{u'_t u'_{t+\tau}}/\overline{u'^2_t} \tag{1}$$

was obtained by means of a delay line, model 802-G1, AD-YU Electronics Lab., Inc., which has a delay time τ adjustable in steps of 2 μsec up to 18 msec and a cut-off frequency of $35/\tau$ for 3 decibel band-width. A delay-line driver was built by the Institute for the purpose of restoring the amplitude of the delayed signal $u'_{t+\tau}$ to its original magnitude and transmitting it with the undelayed signal u'_t to a root-mean-square analyser. The system was calibrated with a known sinusoidal wave from an audio oscillator at successive increments of delay time. The spectrum measurements are presently being repeated with an improved technique and will be reported in the near future.

If the velocity fluctuations of the turbulence are visualized as the result of heterogeneously composed eddies carried along by the mean flow, then there can be distinguished by their function in the energy-transfer process two groups of eddies, each of which is characterized by a significant length scale. In the following, the length scale

$$L = U_0 \int_0^{\tau_0} R_\tau \, d\tau, \tag{2}$$

† Ridjanovic (1963) used the intensities rather than their squares for this correction. All affected data were revised before their application in this paper.

where τ_0 is the smallest delay time at which R_τ becomes zero (see figure 11), is considered representative of the size of those eddies that carry most of the turbulence energy. The dissipation length λ, on the other hand, can be considered roughly indicative of the eddies responsible for the energy dissipation (strictly in the final period only) and can either be evaluated from the spectrum curve or from the measured temporal velocity derivative $\partial u'/\partial t$ through the definition equation

$$\frac{\overline{u'^2}}{\lambda^2} = \overline{\left(\frac{\partial u'}{\partial x}\right)^2} \approx \frac{1}{\bar{u}^2}\overline{\left(\frac{\partial u'}{\partial t}\right)^2}, \tag{3}$$

where the bars indicate temporal averages. Both evaluations are strictly applicable only to isotropic turbulence but can be used here on the assumption of local isotropy within the small-scale structure of turbulence. Because of the difficulties in getting unbiased measurements of $\partial u'/\partial t$, the determination of λ has been postponed until the spectrum measurements are completed.

3. Experimental realization of the flow

A criterion for the experimental realization of the desired wake flow past an axisymmetric, self-propelled body is obtained from the momentum equation. A useful form of this equation is derived by integrating the first equation of Reynolds over a region bounded by a normal reference section with uniform

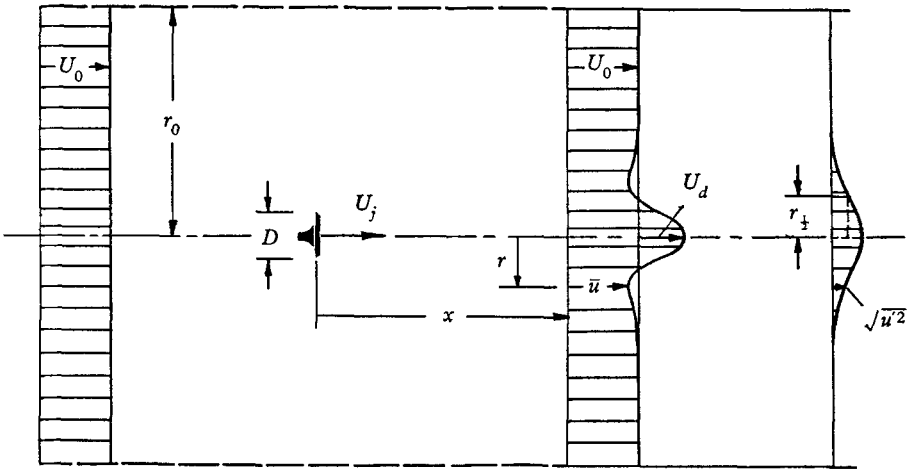

FIGURE 2. Definition sketch.

velocity distribution well upstream from the disk, a normal section at distance x downstream, and a cylindrical surface of radius $r_0 = 5D$ which includes the diffusion zone over the entire range of measurements (see figure 2). If, for high Reynolds numbers, the viscous stress $2\mu\, d\bar{u}/dx$ is neglected in comparison to the normal Reynolds stress $\rho\overline{u'^2}$ and the mean ambient pressure $\bar{p}$ (referred to a zero pressure in the free stream), the resulting equation may be written in the following non-dimensional form

$$2\int_0^{r_0}\left[\left(\frac{\bar{u}}{U_0}\right)^2 - \left(\frac{\bar{u}}{U_0}\right)\right]\frac{r\,dr}{D^2} = -2\int_0^{r_0}\frac{\overline{u'^2}}{U_0^2}\frac{r\,dr}{D^2} - \int_0^{r_0}\frac{\bar{p}}{\frac{1}{2}\rho U_0^2}\frac{r\,dr}{D^2}. \tag{4}$$

No external forces have been included in this equation, because the flow is considered to be unaffected by body forces such as gravity, and because the drag of pipe and disk is balanced by the thrust of the jet.

From a series of exploratory measurements, the average efflux velocity U_j of the jet for which equation (4) was satisfied was found to be $3{\cdot}64U_0$ for the specific apparatus used (Wang 1965). The data obtained from the final measurements with the correct velocity ratio U_j/U_0 have been evaluated by Ridjanovic (1963)

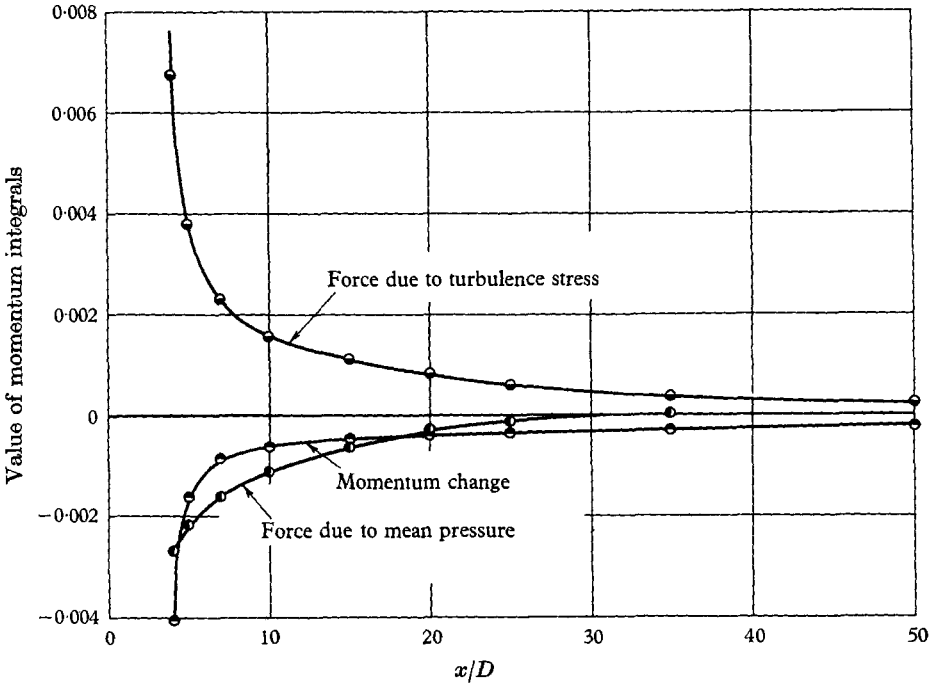

FIGURE 3. Evaluation of experimental data according to momentum integrals of equation (4).

and his results are plotted in figure 3. When corresponding ordinates are summed up according to equation (4), the results do not deviate from the requirement of the equation by more than 0·5 % of the reference momentum flux $\rho\pi(\frac{1}{2}D)^2U_0^2$.

It is interesting to note that the change in momentum flux between the reference section upstream and a section downstream from the body, represented by the left-hand term in equation (4), has a definite magnitude equal to the force produced by the integral of the normal stress $\bar{\sigma}_x = -\bar{p} - \rho\overline{u'^2}$ over any downstream section. Strictly, $\bar{p} \neq 0$, so that the wake of a self-propelled body is not one of zero momentum flux.

4. Experimental results and analysis

4.1. *Energy transformation*

If the experimental results are to give an insight into the overall flow structure and the mechanism of energy transformation, they have to be interpreted in accordance with the equations of motion. Of particular importance in this regard

is the energy equation of the turbulence, which, when expressed in cylindrical co-ordinates x, r, and θ, for a steady, axially-symmetric, mean flow of an incompressible fluid without spiral component and not affected by external forces, reduces to

$$-\rho\left[\overline{u'^2}\frac{\partial\bar{u}}{\partial x}+\overline{v'^2}\frac{\partial\bar{v}}{\partial r}+\overline{w'^2}\frac{\bar{v}}{r}+\overline{u'v'}\left(\frac{\partial\bar{u}}{\partial r}+\frac{\partial\bar{v}}{\partial x}\right)\right]-\left[\frac{\partial}{\partial x}\overline{u'p'}+\frac{1}{r}\frac{\partial}{\partial r}(r\overline{v'p'})\right]$$

$$+\frac{\mu}{r}\left\{r\frac{\partial}{\partial x}\left[\frac{\partial}{\partial x}\left(\frac{\overline{q^2}}{2}\right)+\frac{\partial\overline{u'^2}}{\partial x}+\frac{1}{r}\frac{\partial}{\partial r}(r\overline{u'v'})\right]+\frac{\partial}{\partial r}r\left[\frac{\partial}{\partial r}\left(\frac{\overline{q^2}}{2}\right)+\frac{\partial\overline{u'v'}}{\partial x}+\frac{1}{r}\frac{\partial}{\partial r}(r\overline{v'^2})-\frac{\overline{w'^2}}{2}\right]\right\}$$

$$=\frac{\rho}{2}\left[\bar{u}\frac{\partial\overline{q^2}}{\partial x}+\bar{v}\frac{\partial\overline{q^2}}{\partial r}\right]+\frac{\rho}{2}\left[\frac{\partial}{\partial x}(\overline{u'q^2})+\frac{1}{r}\frac{\partial}{\partial r}(r\overline{v'q^2})\right]+\Delta. \tag{5}$$

The terms of this equation have been so arranged that the left-hand side represents the rate at which work is done per unit volume and the right-hand side the corresponding rate of energy change. The first term signifies the rate at which energy is transferred from the mean motion to the turbulent; so far as the turbulence is concerned, it represents an external supply of energy, as a result of the working of the mean motion against the turbulent stresses. The second and third terms represent the rates at which work is done by the pressure fluctuations and by the viscous stresses in the turbulent motion. The three terms on the right-hand side indicate the rates of change of the turbulence kinetic energy $\frac{1}{2}\rho\overline{q^2}=(\overline{u'^2}+\overline{v'^2}+\overline{w'^2})\frac{1}{2}\rho$ through convection by the mean motion, diffusion by the turbulence, and dissipation into heat by direct action of viscosity. The latter quantity is explicitly expressed as

$$\Delta=\mu\left[2\overline{\left(\frac{\partial u'}{\partial x}\right)^2}+2\overline{\left(\frac{\partial v'}{\partial r}\right)^2}+2\overline{\left(\frac{\partial w'}{r\,d\theta}+\frac{v'}{r}\right)^2}\right.$$

$$\left.+\overline{\left(\frac{\partial u'}{\partial r}+\frac{\partial v'}{\partial x}\right)^2}+\overline{\left(\frac{\partial w'}{\partial x}+\frac{\partial u'}{r\,\partial\theta}\right)^2}+\overline{\left(\frac{\partial w'}{\partial r}+\frac{\partial v'}{r\,\partial\theta}-\frac{w'}{r}\right)^2}\right]. \tag{6}$$

If the Reynolds number of the mean flow $\mathscr{R}_D=U_0D/\nu$ is assumed to be sufficiently high for the mean viscous stresses to be negligible and for the Kolmogoroff approximation

$$\Delta=15\mu\overline{\left(\frac{\partial u'}{\partial x}\right)^2} \tag{7}$$

to apply, and if, furthermore, use is made of the boundary-layer approximations modified for wake flows with slow lateral spreading, then equation (5) assumes the form

$$\frac{\overline{u'v'}}{U_0^2}\frac{\partial\bar{u}/U_0}{\partial r/D}+\frac{1}{2}\frac{\bar{u}}{U_0}\frac{\partial}{\partial x/D}\left(\frac{\overline{q^2}}{U_0^2}\right)+\frac{1}{2r}\frac{\partial}{\partial r/D}r\frac{\overline{v'}}{U_0}\left(\frac{q^2}{U_0^2}+\frac{p'}{\rho U_0^2/2}\right)+\frac{15}{\mathscr{R}_D}\overline{\left(\frac{\partial u'/U_0}{\partial x/D}\right)^2}=0. \tag{8}$$

An integral relationship corresponding to that of the previous momentum analysis is obtained by integration of equation (5) over a cylindrical region of radius r_0 extending downstream from the initial section of measurement at axial

position x_1 to a final section at x; with the same assumptions applied above, the integral form of the turbulence-energy equation becomes

$$4\int_{x_1}^{x}\int_0^{r_0}\frac{\overline{u'v'}}{U_0^2}\frac{\partial\bar{u}/U_0}{\partial r/D}\frac{r\,dr\,dx}{D^3}+2\int_0^{r_0}\frac{\bar{u}}{U_0}\frac{\overline{q^2}}{U_0^2}\frac{r\,dr}{D^2}\Bigg|_{x_1}^{x}$$
$$+2\int_0^{r_0}\left(\frac{\overline{u'q^2}}{U_0^3}+\frac{\overline{u'p'}}{\rho U_0^3/2}\right)\frac{r\,dr}{D^2}\Bigg|_{x_1}^{x}+\frac{60}{\mathscr{R}_D}\int_{x_1}^{x}\int_0^{r_0}\left(\frac{\overline{\partial u'/U_0}}{\partial x/D}\right)^2\frac{r\,dr\,dx}{D^3}=0. \qquad (9)$$

The limits shown on the right-hand sides of the second and third terms indicate that the differences between the respective integrals at axial positions x and x_1 should be evaluated. As follows from the earlier discussion, the successive terms in equations (8) and (9) signify transfer of energy from the mean flow by turbulence production, convection and diffusion of turbulence energy, and viscous dissipation into heat. It should be noted that the diffusion in the axial direction has been neglected in equation (8) but retained in equation (9), because, due to the integration with respect to x, its contribution need not be negligible in the latter equation.

If the turbulence-energy production were concentrated in a point, as in an ideal case of flow past a point source of turbulence, then the last two equations, exclusive of the first terms, would give the complete story about the energy transformation. In the actual case investigated, however, there exists an initial shear régime in which equations (8) or (9) have to be supplemented by the energy equation of the mean motion. In its integral form, approximated by the same assumptions as the turbulence-energy equation, this equation reads

$$2\int_0^{r_0}\left(\frac{\bar{u}}{U_0}\frac{\bar{V}^2}{U_0^2}-\frac{\bar{u}}{U_0}\right)\frac{r\,dr}{D^2}\Bigg|_{x_1}^{x}+2\int_0^{r_0}\frac{\bar{u}}{U_0}\frac{\bar{p}}{\frac{1}{2}\rho U_0^2}\frac{r\,dr}{D^2}\Bigg|_{x_1}^{x}$$
$$+4\int_0^{r_0}\frac{\bar{u}}{U_0}\frac{\overline{u'^2}}{U_0^2}\frac{r\,dr}{D^2}\Bigg|_{x_1}^{x}-4\int_{x_1}^{x}\int_0^{r_0}\frac{\overline{u'v'}}{U_0^2}\frac{\partial\bar{u}/U_0}{\partial r/D}\frac{r\,dr\,dx}{D^3}=0, \qquad (10)$$

where $\bar{V}$ is the resultant mean velocity, which is very nearly equal to $\bar{u}$ within the range of measurements. The production term of equation (9) appears once again, but with a negative sign, for it now represents the rate at which energy is lost by the mean motion over the region considered. The remaining terms represent: the first, the increase in mean energy flux between the initial and final section; the second and third, the cumulative rates at which work is done by the mean pressure and by the turbulence stresses, respectively.

More important than the check upon the general accuracy of measurement is the overall information on the dynamics of the flow that can now be obtained by an evaluation of the data in accordance with these energy equations. Their approximate forms seem justified by the moderately high Reynolds number of around 55,000 and by the observed slow spreading of the diffusion zone ($d\log r_{\frac{1}{2}}/d\log x \ll 1$, see figure 14). A comprehensive discussion of equations (8) and (9) cannot be given before reliable data for the determination of the diffusion and dissipation terms become available from future measurements. Nevertheless, some general conclusions can be drawn from the partial evaluation depicted in figures 4 and 5.

For any point in the wake cross-section represented in figure 4, the local rate of production (first term of equation (8)) is substantially smaller than the corresponding change in convection rate (second term of equation (8)), contrary to conditions in elementary shear flows (Townsend 1949). Of course, figure 4 is only

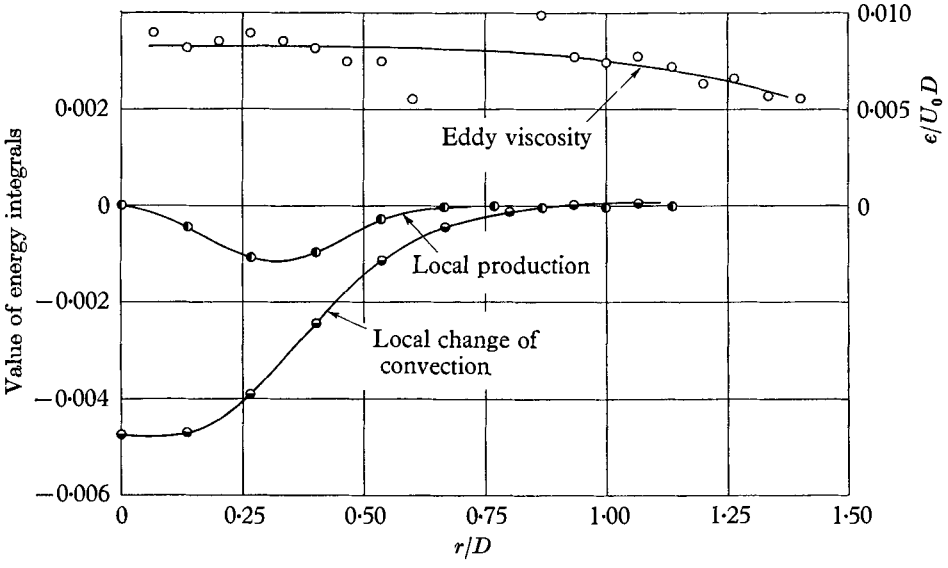

FIGURE 4. Evaluation of experimental data for $x/D = 7$ according to equations (8) and (16).

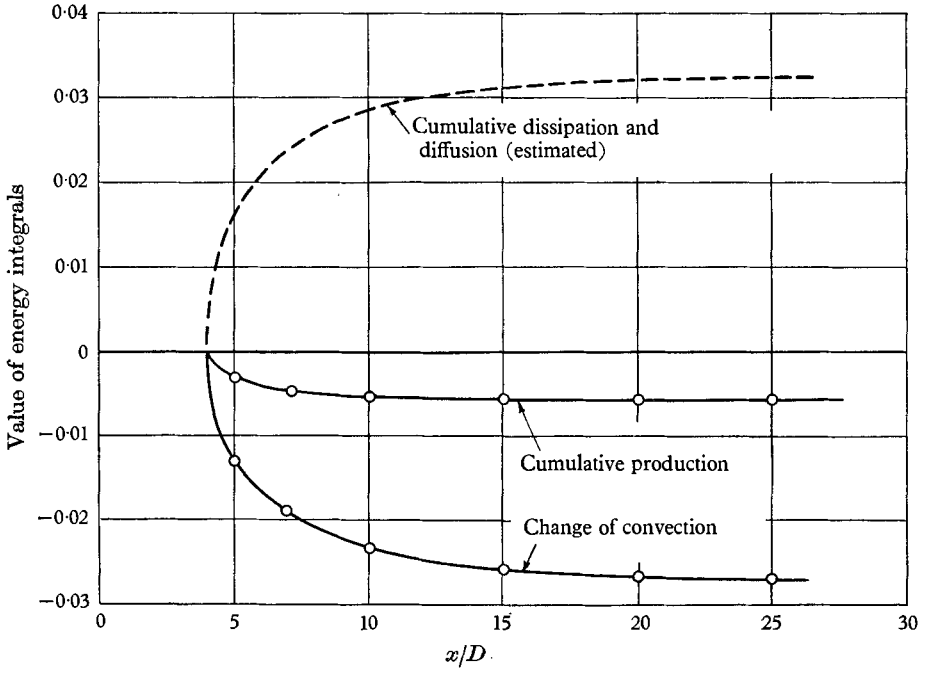

FIGURE 5. Results of turbulence-energy analysis according to equation (9).

representative of a transition from a zone of pronounced shear close to the body to an almost shear-free régime downstream. As becomes evident from figure 5, the cumulative rate of turbulence production approaches a constant value almost within 10 disk diameters. Since this value must be equal to the total rate at which energy is produced by the jet propulsion

$$E_j = \int_0^{\frac{1}{2}d} [\rho(U_j^2 - U_0^2) + 2\bar{p}_e] U_j \pi r\, dr = 5{\cdot}46\rho\pi d^2 U_0^3,$$

where d is the jet diameter and $\bar{p}_e$ the ambient pressure at the jet exit, it follows from figure 5 that all but 0·86 % of this total energy input has already been converted to turbulence-energy upstream from the initial section of measurement. With almost no further production, then, all the turbulence energy that

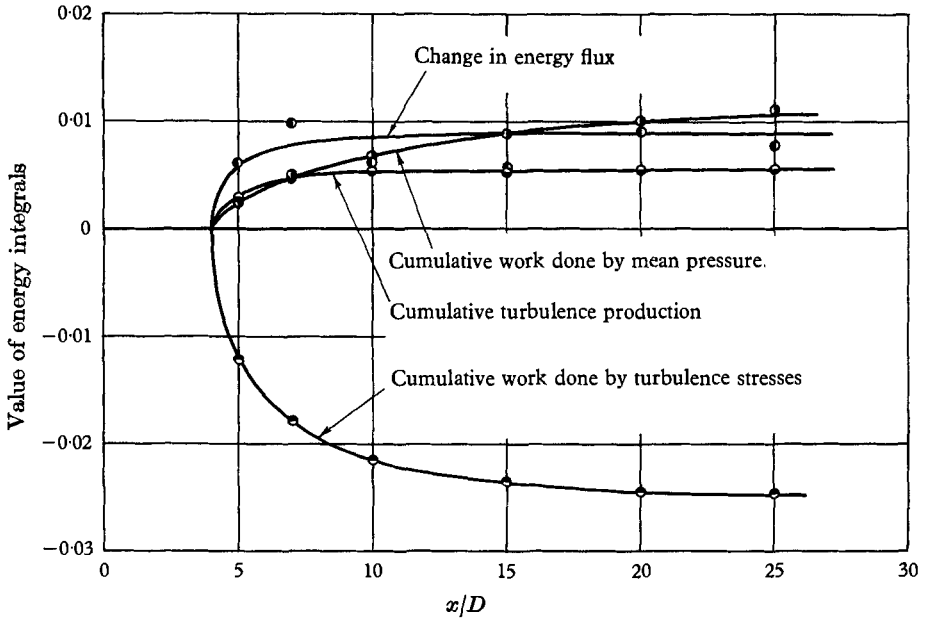

FIGURE 6. Results of mean-energy analysis according to equation (10).

has not been dissipated upstream from $x/D = 10$ is merely being convected and, presumably to a very small extent, diffused downstream for subsequent dissipation into heat. For the correct interpretation of figure 5, it is to be pointed out that the absolute rate of convection (compared to a section upstream from the body) reaches a maximum upstream from the initial section $x_1/D = 4$ and gradually decreases toward zero thereafter; actually depicted in figure 5 is the difference between the rate of convection past the section under consideration and that past the initial section, obviously a negative value. By adding to the convection curve the total rate of turbulence production downstream from the initial section, one obtains the dashed curve, which should chiefly represent the total rate of dissipation over the same region.

From the trend of the curves in figure 5 and their estimated upstream extrapolation, three significant facts can be learned: practically all the turbulence

energy is produced over an extremely limited shear zone; at the beginning of this zone, the turbulence energy is transferred by convection and diffusion at almost the same rate as it is produced, while dissipation only gradually sets in; as the rate of diffusion becomes negligible past the shear zone, the axial rate of change of the cumulative rate of dissipation approaches that of the rate of convection. The last fact in particular distinguishes the investigated flow from elementary shear flows, in which equilibrium is approached between the rates of change of the cumulative dissipation and production rates (compare Rouse 1960).

To complete the description of the overall picture of energy transfer, the mean-energy integrals of equation (10) have been plotted in figure 6 as evaluated by Ridjanovic (1963). While the turbulence stresses do almost no work in producing turbulence beyond $x/D = 10$, they continue to do conservative work, the rate of change of which is balanced by that of the conservative work of the mean pressure. Beyond $x/D = 25$ all the mean-energy integrals attain very nearly constant values. The agreement of the evaluated curves in figure 6 with the requirement of the equation becomes evident from the proximity to the zero line of the sum of corresponding ordinates of the four curves. The scatter of the points, calculated from the first integral of equation (10), is due to the great sensitivity of the integrand to slight errors in the determination of U_0.

4.2. *Variation of flow characteristics*

The actual experimental data of the various flow characteristics in the wake of a self-propelled body, corrected for known bias of instruments and equipment as discussed earlier, are reported by Ridjanovic (1963) and Wang (1965); the velocity difference $\overline{u}_d = \overline{u} - U_0$, the mean pressure $\overline{p}$ referred to the pressure in the undisturbed free stream, and the turbulence characteristics $\overline{u'v'}$, $\overline{u'^2}$, $\overline{v'^2}$, $\overline{w'^2}$, by the former, and the auto-correlation function by the latter. For the following representation of experimental results in table 1 and in figures 7 to 11, points from faired curves through each set of data have been used rather than the measurements themselves, and all values have been reduced to a non-dimensional form through division by suitable reference magnitudes. Four of these magnitudes, namely, $U_d = (\overline{u}_d)_{\max}$, $u'_{\max}$, the radial distance $r_{\frac{1}{2}}$ at which the axial turbulence intensity u' equals half of its maximum value, and the integral scale L as defined by equation (2) will play important roles as velocity and length scales in the approximate analysis of the experimental results (hereafter, mean-square and root-mean-square symbols are reduced to u'^2 and u' where this does not lead to misinterpretation). The relative axial distance from the disk $x_0/D = 2$ at which the extrapolated curve of $U_0^2/u'^2_{\max}$ was found to intersect the abscissa x has been adopted as virtual origin—a point which can be considered a virtual source of turbulence of infinite intensity and zero scale.

The approximate analysis of the variation of flow characteristics has been based on the hypotheses of Reynolds-number similarity and self-preservation, both of which are similar in principle to the hypotheses used in the analyses of homogeneous turbulence and elementary turbulence-shear flows (Townsend 1956) yet are significantly different in form. The concepts of the development of

the turbulence structure which underlie the two hypotheses are, indeed, no less applicable to the flow under consideration: First, the turbulence or eddy motion is generated by inertial instabilities in the mean flow and governed by inertial interaction of the eddies, so that viscosity should affect only the dissipative components of the motion, which contain relatively little energy provided $\mathscr{R}_D$ is

$\frac{x}{D}$	$\frac{x-x_0}{D}$	$\frac{10^2\overline{p}_{\min}}{\frac{1}{2}\rho U_0^2}$	$\frac{U_d}{U_0}$	$10^2\frac{\overline{u'v'}_{\max}}{U_0^2}$	$\frac{u'_{\max}}{U_0}$	$\frac{v'_{\max}}{U_0}$	$\frac{w'_{\max}}{U_0}$	$10^2\frac{\overline{q^2}_{\max}}{U_0^2}$	$\frac{r_{\frac{1}{2}}}{D}$
4	2	−7·36	0·363	1·620	0·246	0·198	0·193	13·70	0·515
5	3	−4·10	0·252	0·656	0·163	0·127	0·124	5·808	0·60
7	5	−2·10	0·134	0·307	0·110	0·0993	0·0988	3·172	0·72
10	8	−1·05	0·059	0·131	0·0745	0·0700	0·0660	1·481	0·875
15	13	−0·385	0·0277	0·051	0·0535	0·0452	0·0446	0·689	1·025
20	18	−0·27	0·0149	0·024	0·0425	0·0355	0·0335	0·418	1·12
25	23	—	0·0092	0·014	0·0330	0·0310	0·0280	0·283	1·21
35	33	—	—	0·0065	0·0239	0·0232	0·0217	0·158	1·35
50	48	—	—	—	0·0170	0·0162	0·0151	0·078	1·52

TABLE 1

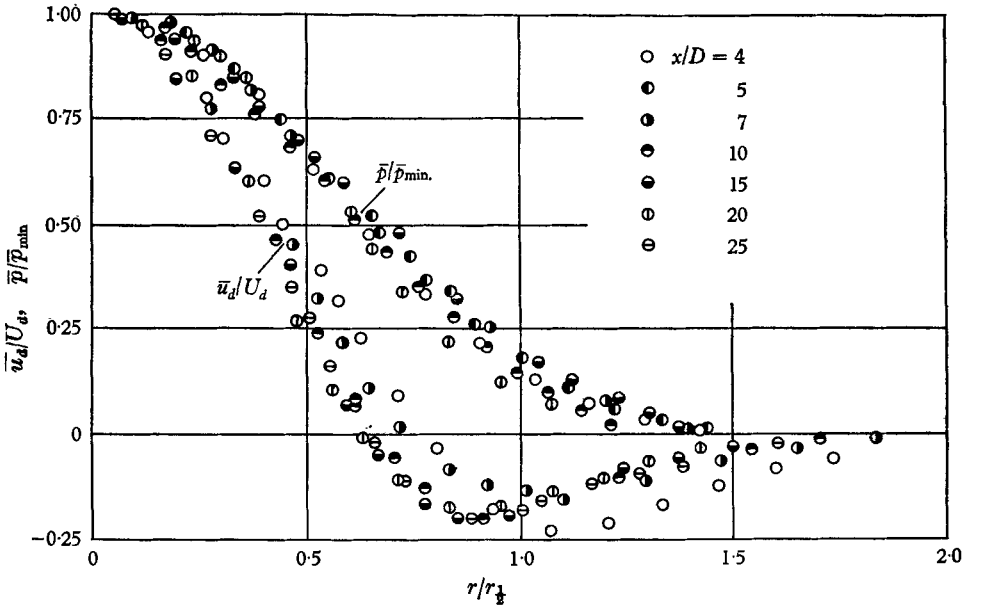

FIGURE 7. Radial variation of mean-flow characteristics in the wake of a self-propelled body.

large. Secondly, as the eddies are carried along by the mean flow within a relatively narrow region, their structure is likely to approach a state of moving equilibrium as it has been continuously developing from earlier ones. Even though turbulence continues to be produced by the mean motion within an initial shear régime, the interrelation between turbulent and mean-flow patterns is so strong—the former being a product as well as a source of change for the latter—

that both flow patterns may be expected to attain asymptotically self-preserving forms that are independent of the Reynolds number and the particular initial conditions of flow generation.

Although the propositions for the application of the hypotheses are thus given, the final justification has to come from experiments. As far as the flow characteristics plotted in figures 7–10 are concerned, one is inclined to affirm the existence

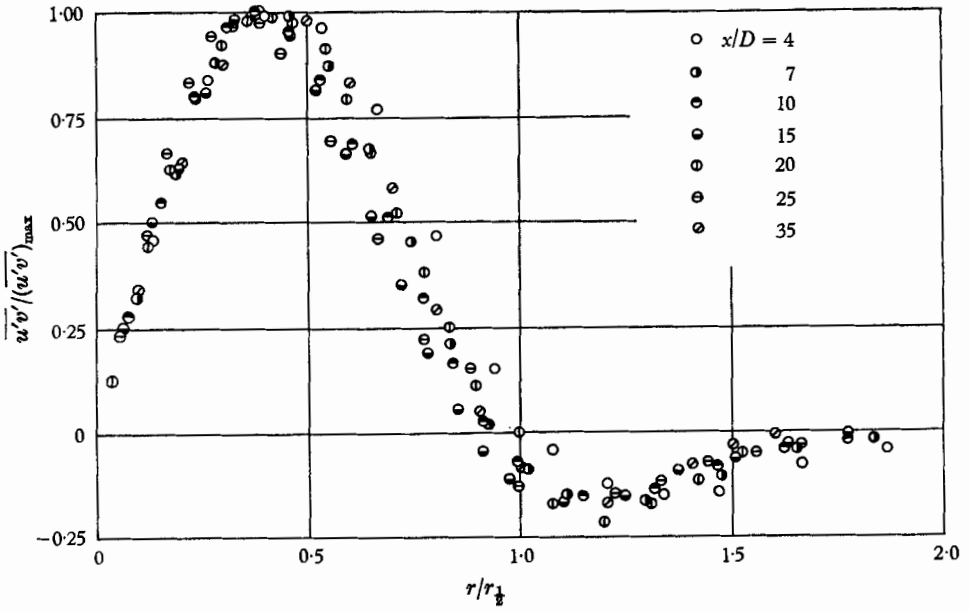

FIGURE 8. Radial variation of turbulent shear.

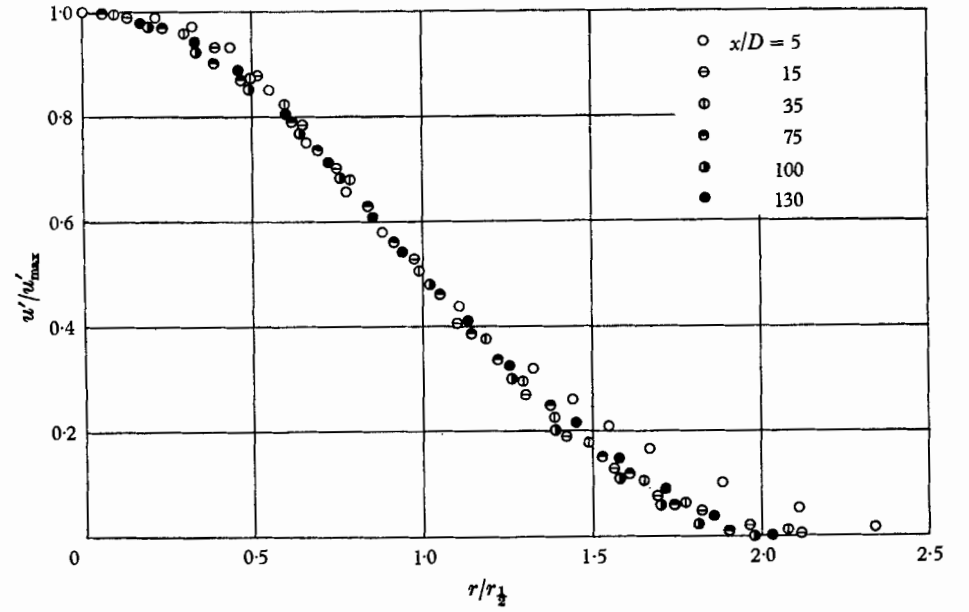

FIGURE 9. Radial variation of axial turbulence intensity.

of self-preserved profiles. Ridjanovic (1963) reports a change in the shape of the mean-velocity profile only for $x/D = 50$. However, the measurements at this station were almost of the order of the estimated experimental error and are

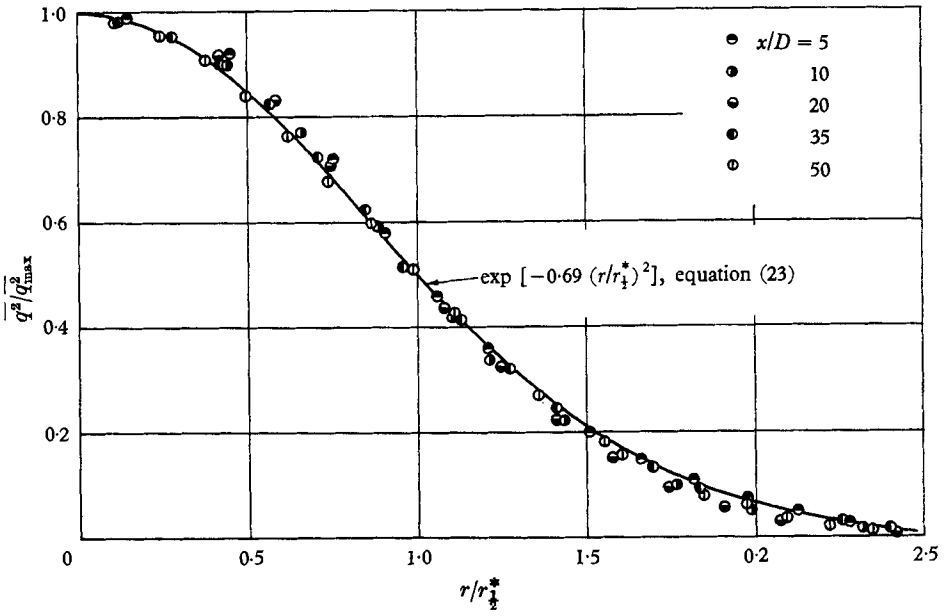

FIGURE 10. Radial variation of turbulence energy.

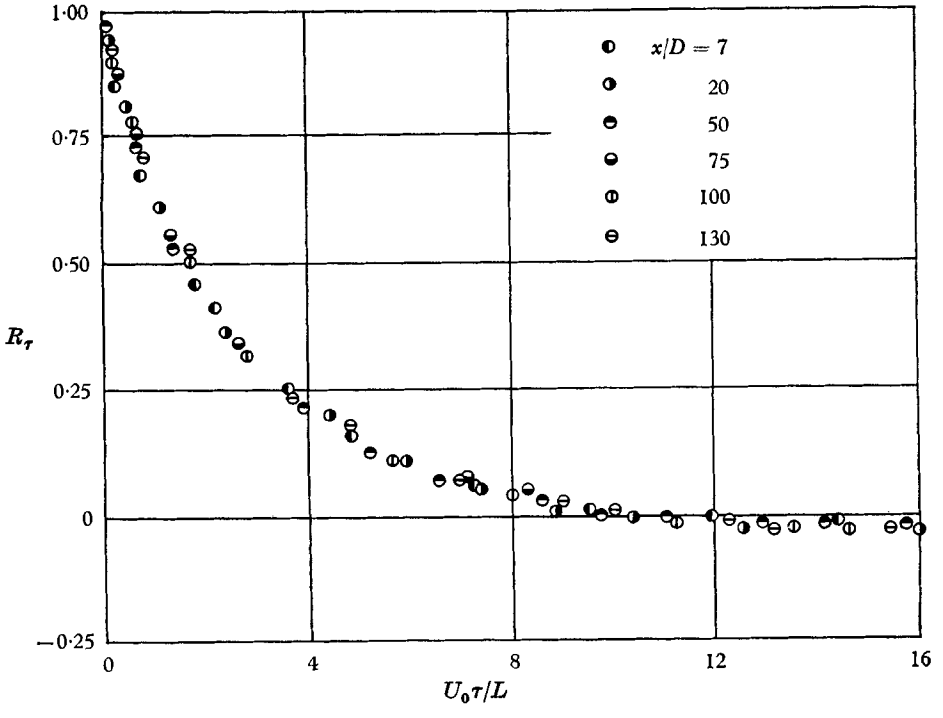

FIGURE 11. Auto-correlation function of the axial-velocity fluctuation.

therefore inconclusive. In regard to the deviations of the turbulence-intensity profiles from a self-preserved shape, one must bear in mind that the background turbulence in the air tunnel had an increasing effect downstream as the ratio of its relative intensity to $u'_{\max}/U_0$ grew to as much as 40 % at $x/D = 130$. In view of this fact, the self-preservation of the profiles in figure 9 is most remarkable. With the experimental scatter minimized by plotting the sum of the three measured quantities $\overline{q^2} = \overline{u'^2} + \overline{v'^2} + \overline{w'^2}$ in figure 10, a self-preserved profile is even more clearly discernible ($r^*_{\frac{1}{2}}$ is the radial distance at which $\overline{q^2}$ equals half of its maximum value).

The notable difference between the self-preserved profiles for simple jets and wakes and those for the specific jet-wake investigated lies in the number of scales necessary to normalize these profiles or describe them analytically. While one pair of scales (velocity and length) proved to be sufficient in the former case, two pairs are required in the latter—one (U_d and $r_{\frac{1}{2}}$) characterizing the inhomogeneity and one ($u'_{\max}$ and L) the structure of turbulence. Even though other quantities have been used in the following sections and in figures 7, 8, and 10, they all can be expressed in terms of these four scales, as will be shown below.

4.2.1. *The shear régime*

In accordance with the hypothesis of Reynolds-number similarity, the cross-sectional variations of all flow characteristics should be independent of the Reynolds number. By the definition of self-preservation in its more general form, moreover, they should be expressible non-dimensionally as universal functions of a relative radial position $\eta = r/r_{\frac{1}{2}}$ through suitable kinematic and dynamic scales, i.e.

$$\overline{u}_d/U_d = f(\eta), \quad \overline{p}/\overline{p}_{\min} = g(\eta), \quad \overline{u'^2}/\overline{u'^2_{\max}} = h(\eta), \quad \overline{u'v'}/\overline{(u'v')}_{\max} = k(\eta). \tag{11}$$

These functions are subject to restrictions imposed by the momentum and energy equations. For a region of flow in which (*a*) the distributions of flow characteristics are independent of Reynolds number and self-preserved as defined by equations (11), (*b*) the viscous stresses are small compared to the turbulent stresses, and (*c*) the velocity difference $\overline{u}_d = \overline{u} - U_0$ is small compared to U_0, the momentum equation simplifies to

$$U_d U_0 r_{\frac{1}{2}}^2 \int_0^\infty f\eta\, d\eta + \frac{1}{\rho}\overline{p}_{\min} r_{\frac{1}{2}}^2 \int_0^\infty g\eta\, d\eta + u'^2_{\max} r_{\frac{1}{2}}^2 \int_0^\infty h\eta\, d\eta = 0, \tag{12}$$

and the mean energy equation, derived from the first Reynolds equation for the purpose of this analysis, becomes

$$\begin{aligned}
&\frac{d}{dx}\left[U_0 U_d^2 r_{\frac{1}{2}}^2 \int_0^\infty f^2\eta\, d\eta\right] - 2U_d(\overline{u'v'})_{\max} r_{\frac{1}{2}} \int_0^\infty k \frac{df}{d\eta}\,\eta\, d\eta \\
&\quad + \frac{1}{\rho}\overline{p}_{\min} U_d \frac{d(r_{\frac{1}{2}})^2}{dx} \int_0^\infty g \frac{df}{d\eta}\,\eta^2\, d\eta + 2\frac{d}{dx}\left[\frac{1}{\rho}\overline{p}_{\min} U_d r_{\frac{1}{2}}^2 \int_0^\infty gf\eta\, d\eta\right] \\
&\quad + u'^2_{\max} U_d \frac{d(r_{\frac{1}{2}})^2}{dx} \int_0^\infty h \frac{df}{d\eta}\,\eta^2\, d\eta + 2\frac{d}{dx}\left[u'^2_{\max} U_d r_{\frac{1}{2}}^2 \int_0^\infty hf\eta\, d\eta\right] = 0.
\end{aligned} \tag{13}$$

Since these relations between the universal functions must be true for all values of x, and since each of the integrals is a numerical constant, the coefficients of the integrals should be either zero or proportional to each other. The conditions for a self-preserving flow are, hence,

$$\overline{p}_{\min}/\rho U_0 U_d = \text{const.}, \tag{14a}$$

$$u'^2_{\max}/U_0 U_d = \text{const.}, \tag{14b}$$

and

$$\frac{U_0 U_d}{(\overline{u'v'})_{\max}} \frac{dr_{\frac{1}{2}}}{dx} = \text{const.}, \tag{15a}$$

$$\frac{U_d}{r_{\frac{1}{2}}} \frac{dr_{\frac{1}{2}}/dx}{dU_d/dx} = \text{const.} \tag{15b}$$

A reduction of the reference scales in equation (11) to the significant velocity and length scales U_d, $u'_{\max}$, $r_{\frac{1}{2}}$, and L is achieved through equation (14*a*) and, so far as $(\overline{u'v'})_{\max}$ is concerned, by means of the Boussinesq assumption

$$\overline{u'v'} = -\epsilon \frac{\partial \overline{u}_d}{\partial r}. \tag{16}$$

With the predominant part of the turbulent movements (i.e. the part containing most of the turbulence energy) in a quasi-equilibrium state as proposed earlier, it is reasonable to expect that the eddy viscosity ϵ should depend only on the velocity and length scales u^* and L characterizing these movements. On dimensional grounds then, $\epsilon/(Lu^*)$ should be a constant throughout the diffusion zone. If the intermittent character of the flow due to the sharply separated regions of turbulent and non-turbulent fluid were taken into account, a velocity scale characteristic of the turbulent fluid would be roughly $u^* = \sqrt{(\overline{u'^2}/\gamma)}$, where γ is the intermittency factor; however, it is well within the accuracy of this theory to assume $u^* \sim u'_{\max}$. With the additional, experimentally verified assumption that L is constant over any cross-section, $\epsilon \sim Lu'_{\max}$ becomes independent of r (which in itself is verified by the plot in figure 4), and $(\overline{u'v'})_{\max}$ can finally be expressed as

$$(\overline{u'v'})_{\max} = -\epsilon \frac{U_d}{r_{\frac{1}{2}}} \left(\frac{df}{d\eta}\right)_{\max} \sim Lu'_{\max} \frac{U_d}{r_{\frac{1}{2}}}. \tag{17}$$

Herewith, the alternative form of equation (15) becomes

$$\frac{r_{\frac{1}{2}} U_0}{Lu'_{\max}} \frac{dr_{\frac{1}{2}}}{dx} = \text{const.} \tag{18}$$

A further reduction in generality of the universal functions—for example, the replacement of the scale u^* by U_d, as has been customary to date—would not be compatible with the experimental results.† Therefore, the equations of momentum and mean energy merely provide necessary conditions for the axial variations of the scales rather than their solution.

† For $(\overline{u'v'})_{\max} \sim U_d^2$, equation (15*a*) would yield $U_d \sim d(r_{\frac{1}{2}})/dx$, which is not verified by the experiments. The total turbulence is apparently less closely connected with the local mean-flow conditions than in cases of elementary free-turbulence shear flows; in the latter, $\overline{u'v'}$ as well as $\overline{u'^2}$ were found to have self-preserved profiles when related to U_d^2.

In order to check the validity of the analysis, the parameters of equations (14), (15), and (18) were evaluated from the experimental data in tables 1 and 3; from their representation in table 2 it is evident that, as predicted, the parameters of equations (14) and (18) vary only little, apparently at random, and the parameters of equation (15) tend toward constant values.

$\frac{x}{D}$	Parameter of equations					
	(14*a*)	(14*b*)	(15*a*)	(15*b*)	(18)	(35)
5	−0·40	9·5	3·0	−0·36	1·8	0·48
7	−0·33	11·1	2·4	−0·26	1·9	0·51
10	−0·31	10·6	1·8	−0·20	2·1	0·54
15	−0·36	9·7	1·14	−0·14	1·6	0·40
20	−0·28	8·3	1·09	−0·12	1·7	0·41
25	−0·36	8·5	1·02	−0·12	1·9	0·47

TABLE 2

It can be shown that the conditions expressed by equations (14), (15), and (18) also hold for the state of self-preservation in the wake of a self-propelled two-dimensional body or a line source of turbulence. The most interesting result is that the mean velocity difference decays in proportion to the square of the velocity fluctuation.

4.2.2. *The shear-free régime*

No use has yet been made of the turbulence-energy relationship. Even in the simplified form of equation (8), however, this relationship does not lend itself to analysis without additional approximations. The greatest obstacle to analysis is the sum of the two terms in the third expression of equation (8). Although each plays a similar role in transporting turbulence energy from one part of the flow to another, there exists no similarity in their relation to local or overall flow conditions, nor does there necessarily exist a relation between them (Townsend 1956). It is therefore a drastic simplification to assume the combined terms to be proportional to the local gradient of turbulence energy. Nonetheless, this proportionality is adopted here, because it leads to the mathematically simplest form which is still physically plausible, at least so far as the energy-velocity term is concerned,

$$\overline{v'(\tfrac{1}{2}q^2+p'/\rho)} = -\epsilon_e(\partial/\partial r)(\tfrac{1}{2}\overline{q^2}). \tag{19}$$

The factor of proportionality ϵ_e in this expression may be designated as an energy-diffusion coefficient in analogy to the coefficient ϵ for momentum diffusion in equation (16).

If the analysis is restricted to the downstream region of negligible shear and nearly uniform mean velocity distribution, and if the experimental observations are applied, that (*a*) the components of the turbulence intensities become almost equal, i.e. $\overline{u'^2} = \frac{1}{3}\overline{q^2}$ (see table 1, columns 6 and 9), and (*b*) the dissipation length λ defined by equation (3) is independent of the radial position, equation (8) can be written as

$$U_0\frac{\partial\overline{u'^2}}{\partial x} - \frac{1}{r}\frac{\partial}{\partial r}\left(r\epsilon_e\frac{\partial\overline{u'^2}}{\partial r}\right) + 10\nu\frac{\overline{u'^2}}{\lambda^2} = 0. \tag{20}$$

For flow which is self-preserving in accordance with equation (11 *c*), this equation, when integrated over a cross-sectional plane from the centre-line to a circle outside the diffusion zone and divided by the constant $\int h\eta\, d\eta$, yields

$$\frac{10\nu}{U_0\lambda^2} = -\frac{du'^2_{\max}/dx}{u'^2_{\max}} - \frac{d(r_{\frac{1}{2}})^2/dx}{(r_{\frac{1}{2}})^2}, \tag{21}$$

because the integral of the second term of equation (20) is zero at both integration limits. Through equations (11) and (21), equation (20) finally leads to the differential equation for $h(\eta)$

$$\frac{dh}{d\eta} + \left(\frac{U_0 r_{\frac{1}{2}}}{\epsilon_e}\frac{dr_{\frac{1}{2}}}{dx}\right)\eta h = 0, \tag{22}$$

in which the diffusion coefficient ϵ_e may still be a function of both x and $\eta = r/r_{\frac{1}{2}}$.

In order to proceed, it will be assumed that $\epsilon_e \sim Lu'_{\max}$ on the basis of similar arguments as used for the specification of ϵ. This assumption has two significant consequences: first, since none of the terms within the parentheses of equation (22) varies with η, and since their combination must be invariant with x for this equation to be identically satisfied, the parenthetic expression must be a constant—a condition already obtained by equation (18); second, $h(\eta)$ becomes a Gaussian error function—a result which is contained in the complete solution of equation (20), i.e.

$$\overline{u'^2} = \tfrac{1}{3}\overline{q^2} = \frac{A}{\int \epsilon_e dx}\exp\left(-\int \frac{10\nu}{U_0\lambda^2}\,dx\right)\exp\left(-\frac{U_0}{4\int \epsilon_e dx}\,r^2\right), \tag{23}$$

and is well confirmed by the experiment (see figure 10). Although the variation of $\overline{q^2}$ with x is included in this solution, it cannot be evaluated without knowledge of $\lambda(x)$.

The counterparts of equation (21) for flows past a line source and a plane source of turbulence are derived in a similar manner as

$$\frac{10\nu}{U_0\lambda^2} = -\frac{du'^2_{\max}/dx}{u'^2_{\max}} - \frac{dy_{\frac{1}{2}}/dx}{y_{\frac{1}{2}}} \tag{24}$$

and

$$\frac{10\nu}{U_0\lambda^2} = -\frac{du'^2/dx}{u'^2}, \tag{25}$$

respectively. They reveal the influence which different degrees of diffusion-zone spreading have on the decay of turbulence energy and will be used for comparison in the following chapter. The form of and conclusions drawn from equation (22) remain unchanged for flow past a line source of turbulence.

4.2.3. *Power-law approximations*

For both the shear and the shear-free régimes, a complete prediction of the axial variation of flow characteristics is not possible with the equations presented unless they are supplemented by additional hypotheses. Although such prediction is bound to become less rigorous with each hypothesis, it is still worth pursuing. Beside the obvious advantage of an analytical tool, it provides,

through comparison with experimental results, an indication as to which one of different possible dynamical concepts (on which the hypotheses are based) applies most closely to the flow under consideration. In the following, two approaches will be presented, one utilizing and one avoiding the power-law approximations that have become standard in the analyses of free-shear flows and grid turbulence.

As a matter of fact, the system of simultaneous equations (14), (15), and (17), combined with hypothesis (*b*) below, does yield power laws in x as solutions for the unknown functions, at least so far as the shear régime is concerned. Suppose, then, power laws are adopted for the entire field of flow, i.e.

$$U_d/U_0 = C_1[(x-x_0)/D]^n,\ \overline{p}_{\min}/\tfrac{1}{2}\rho U_0^2 = C_2[(x-x_0)/D]^{n^*},\ u'^2_{\max}/U_0^2 = C_3[(x-x_0)/D]^{n'},$$
$$(\overline{u'v'})_{\max}/U_0^2 = C_4[(x-x_0)/D]^{n''},\quad r_{\frac{1}{2}}/D = C_5[(x-x_0)/D]^m,\quad L/D = C_6[(x-x_0)/D]^{m'}, \tag{26}$$

in which C_{1-6} are constants within the various zones and the axial position is referred to the virtual origin at $x = x_0$. As a consequence, the conditions of self-preservation for the shear régime, contained in equations (14), (15*a*), and (18), take the forms

$$n'-n = 0,\quad n^*-n = 0, \tag{27}$$

$$n-n''+m-1 = 0, \tag{28}$$

$$n'-4m+2m'+2 = 0, \tag{29}$$

which are equally valid for both point and line sources of turbulence. The last of these equations can also be deduced from equation (22) and therefore applies to the shear-free régime as well.

It is for the shear-free régime that progress in the analysis can be achieved through the supplementary conditions, obtained for a point source and a line source by substituting equation (26) into equations (21) and (24)

$$\left.\begin{aligned}\lambda^2 &= -\frac{10}{n'+2m}\frac{\nu}{U_0}(x-x_\lambda)\\ \text{and}\qquad \lambda^2 &= -\frac{10}{n'+m}\frac{\nu}{U_0}(x-x_\lambda)\end{aligned}\right\} \tag{30}$$

if these conditions† are combined with the assumptions that:

(*a*) Corresponding zones of decay for different sources of turbulence are characterized by similar variations of λ with x, i.e. by similar values of $U_0\lambda^2/[\nu(x-x_\lambda)]$, and

(*b*) Loitsiansky's parameter is invariant along the x-axis.

The first assumption seems reasonable on the basis that some similarity between the flows considered can be expected with respect to the structure of the finer, locally isotropic turbulent movements. Less justified seems to be the second, in that Loitsiansky (1945) derived the invariance of the parameter

$$u'^2\int_0^\infty s^4 R\,ds,$$

† It is one of the inconsistencies of the power-law approach that the axial position x_λ at which $\lambda = 0$ is different from x_0 (compare Batchelor & Townsend 1948*a*, *b*). The condition for a plane source of turbulence equivalent to equation (30) follows from either of these equations through $m = 0$.

(where u'^2R is the two-point velocity correlation and s is the distance between the points) under propositions which, as was shown by Batchelor & Proudman (1956), do not strictly apply even to homogeneous turbulence except in the final zone of decay. Nevertheless, Loitsiansky's invariance condition was experimentally verified by Stewart & Townsend (1951) for the initial zone of decay as well and was repeatedly used with satisfactory results in the derivation of decay laws for this zone, e.g. by Kolmogoroff (1941) and Frenkiel (1948). It is on a similar empirical basis that the invariance of the parameter

$$(u'^2L^5)_{\tau=0}\left[\int_0^\infty \left(\frac{U_0\tau}{L}\right)^4 R_\tau \frac{U_0 d\tau}{L}\right]_{\tau=0} = \text{const.} \tag{31}$$

in which R_τ and $U_0\tau$ replace R and s, respectively, is now postulated for the inhomogeneous turbulence behind a point or a line source. For the point source of turbulence this postulate is verified in figure 11 by the self-preserved shape of the auto-correlation function R_τ, which makes the integral in equation (31) invariant, and in table 3 by the tendency toward a constant value of the factor $(u'^2L^5)_{\tau=0}$.

x/D	L/D	$[10^6u'^2L^5/(U_0^2D^5)]_{\tau=0}$
7	0·20	3·9
20	0·31	5·1
50	0·34	1·8
75	0·40	1·35
100	0·43	1·4
130	0·50	1·35

TABLE 3

With hypotheses (*a*) and (*b*), equations (29) and (30) can finally be evaluated by adopting the values 10 and 7 for $U_0\lambda^2/[\nu(x-x_\lambda)]$ in the initial and intermediate zones of decay, in accordance with the theory of homogeneous turbulence (e.g. Batchelor & Townsend 1948*a*, *b*). Moreover, the trends of flow development can be estimated for 'semi-final' zones, defined here as regions in which the flow processes are still predominantly inertial so that equation (20), the basis for equations (30) and (31), still applies, yet regions which are close enough to the final zone that the proportionality $L \sim \lambda$, characteristic of this zone, has already been approached. The corresponding values of $U_0\lambda^2/[\nu(x-x_\lambda)]$ for the point source and the line source of turbulence are obtained as 4·44 and 4·21 with the aid of equation (30), or as 5·71 and 5·41 if, in analogy to the findings of Batchelor & Stewart (1950), $\overline{u'^2} = (\frac{3}{7})\overline{q^2}$ is introduced instead of assumption (*a*) of the § 4.2.2 but local isotropy in the small-scale motion is assumed to prevail.

The results listed in table 4 for the initial zones past a point source and a line source of turbulence are to be used with reservation, because the influence of turbulent shear, which was neglected in the derivation of equation (30), may still be appreciable and the empirical condition of equation (31) may not yet apply. Nevertheless, for an initial as well as for an intermediate zone, fair agreement with respect to order of magnitude and trend is obtained between the slopes of

the logarithmic plots in figures 14 and 15 and the predicted exponents for respective power laws in table 4. While the predicted exponents for $r_{\frac{1}{2}}(x)$ are slightly smaller than the corresponding power-law trend of $u'_{\max}$ would require, the predicted exponents for $L(x)$ are slightly larger—as is evident from a comparison of the power-law trend of the data for L listed in table 3 with the respective prediction of table 4.

		Exponent of x for the power-law development of										
		Point source				Line source				Plane source		
Zone	$\frac{U_0\lambda^2}{\nu(x-x_\lambda)}$	$\mathscr{R}_\lambda$	$u'_{\max}$	L	$r_{\frac{1}{2}}$	$\mathscr{R}_\lambda$	$u'_{\max}$	L	$y_{\frac{1}{2}}$	$\mathscr{R}_\lambda$	u'	L
Initial	10	−0·27	−0·77	0·31	0·27	−0·15	−0·65	0·26	0·305	0	−0·50	0·20†
Intermediate	7	−0·435	−0·935	0·375	0·22	−0·34	−0·84	0·335	0·25	−0·214	−0·715	0·286‡
Semi-final	—	−0·75	−1·25	0·50	0·125	−0·75	−1·25	0·50	0·125	—	—	—
Final	4	—	—	—	—	—	—	—	—	−0·75	−1·25	0·50

† According to Stewart & Townsend (1951), based on Loitsiansky's invariant.
‡ According to v. Kármán & Howarth (1938), based on Loitsiansky's invariant.

TABLE 4

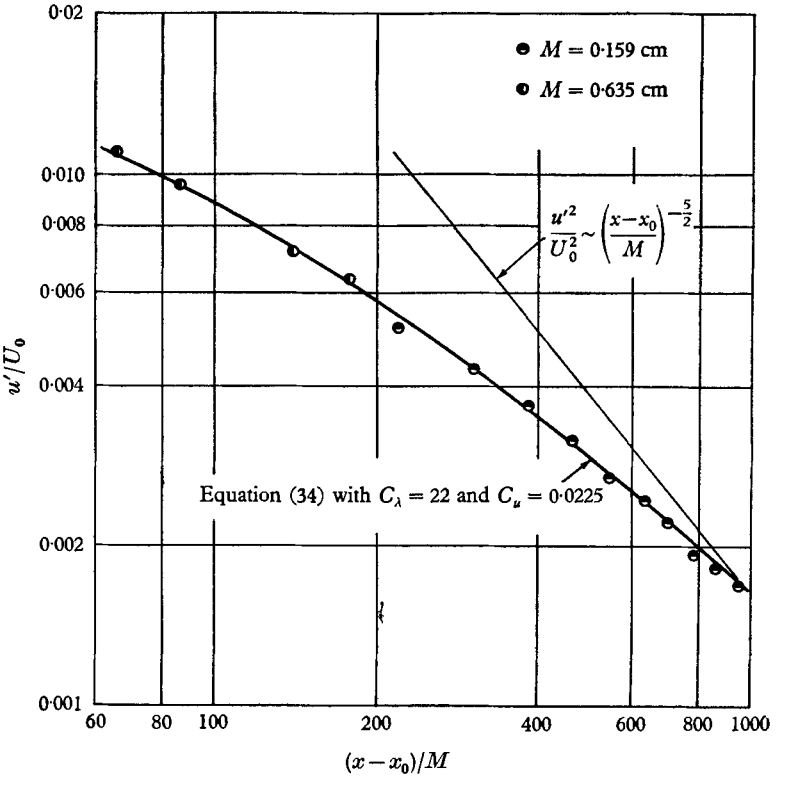

FIGURE 12. Comparison of the trend of equation (34) with data of Batchelor & Townsend (1948*b*) for grid turbulence at $\mathscr{R}_M = 650$.

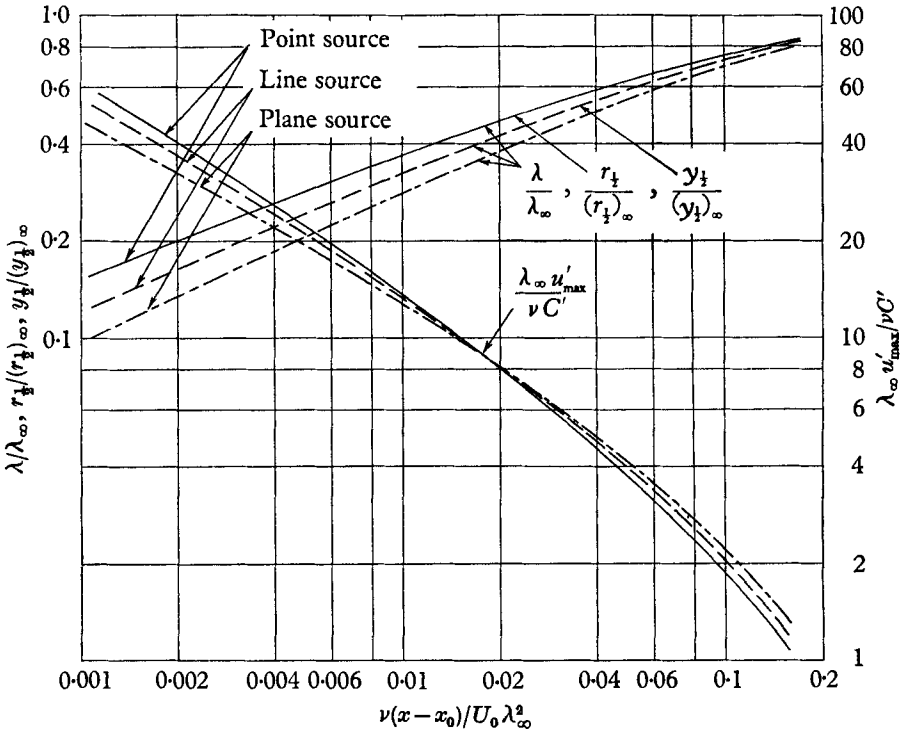

FIGURE 13. Graphical representation of equations (38) and (39).

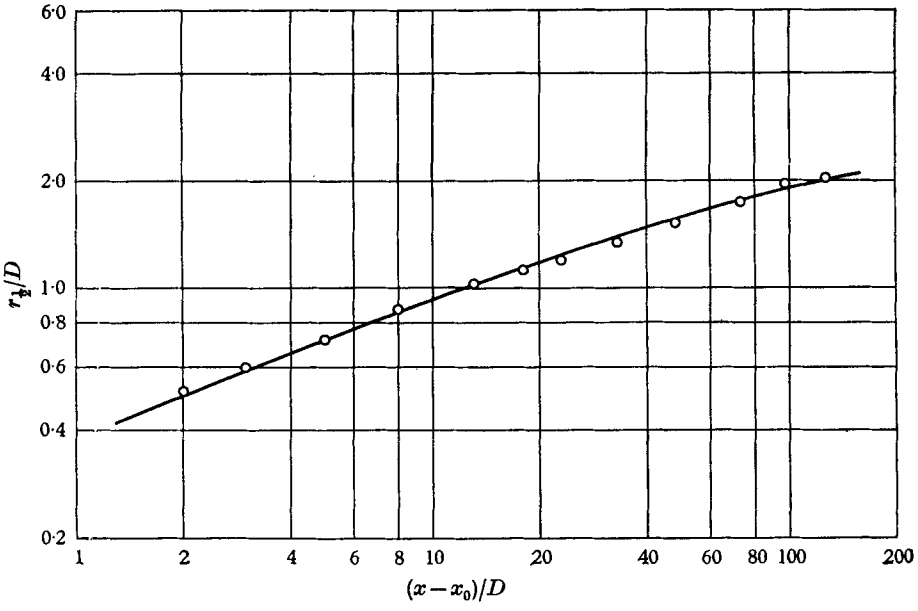

FIGURE 14. Variation of wake width behind a self-propelled body.
——, Equation (38*a*) with $\lambda_\infty/D = 0{\cdot}135$ and $(r_{\frac{1}{2}})_\infty/D = 2{\cdot}5$.

The value of table 4 lies in the fact that it permits direct confrontation of the laws of flow development for the different sources of turbulence with the familiar laws of decay of homogeneous turbulence behind a grid. It is to be noted, however, that, in accordance with the different rates of turbulence-energy decay, the final zones are more or less rapidly approached so that the zones listed in table 4 by no means signify equivalent portions of the flows considered; any zone past a point source of turbulence is expected to be smaller in extent than the corresponding zone past a line or a plane source, provided the Reynolds numbers of the flows are comparable.

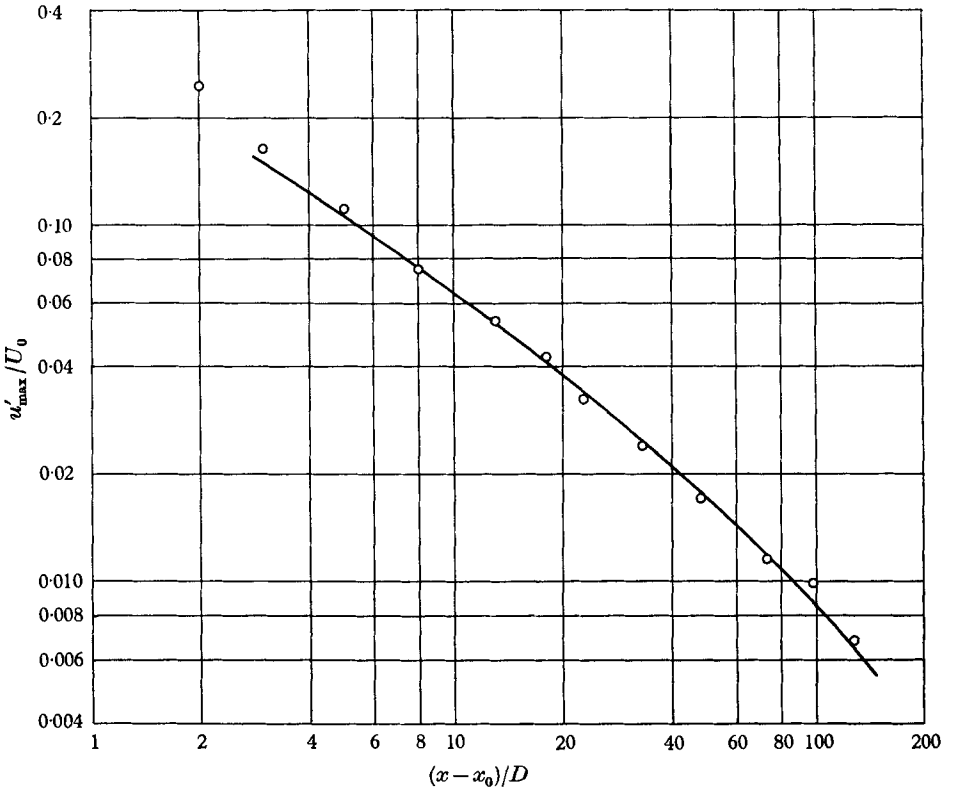

FIGURE 15. Variation of maximum turbulence intensity behind a self-propelled body. ——, Equation (39*a*) with $\lambda_\infty/D = 0{\cdot}135$ and $C' = 35{\cdot}6$.

The greatest distinction between the flows behind different sources of turbulence, of course, is the difference in the freedom of lateral spreading, the effect on the flow development of which is reflected clearly in table 4. The similarities in flow generation and structure, on the other hand, seem significant enough to warrant extension of the presently accepted concepts of the dynamics of decaying homogeneous turbulence to all these flows. In either case, production of turbulence is limited essentially to a short zone of flow establishment which is characterized by disturbed and strained mean flow. Predominantly large-scale eddies are generated in this zone, of the order of the linear dimensions of the turbulence generator. In a following 'initial' zone, energy is transferred by

inertial interaction to other scales which are smaller on the average because of the cascade process set up by viscous dissipation in the smallest eddies. If the Reynolds number of the flow is high enough for the dissipating eddies to be so reduced in scale that they contain only a negligible amount of the turbulence energy, then there will be a range of eddies which are not influenced by viscosity and may therefore attain a state of equilibrium. The equilibrium is not absolute, since the turbulence energy contained in this range diminishes gradually as the external supply of energy tends toward zero; and it cannot persist, since the condition of energy supply from outside of the equilibrium range changes according to laws which are not subject to and consequently do not satisfy the requirements of this range. An 'intermediate' zone is approached when there is no longer a distinction between energy-containing and large-scale eddies; it ends when the turbulence energy, or the Reynolds number of turbulence $\mathscr{R}_\lambda = \lambda u'_{\max}/\nu$, has decreased to the extent that inertial effects become negligible. With the smaller eddies decaying more rapidly than the larger eddies, a stable distribution over a limited size range of non-interacting eddies is reached in a 'final' zone. These eddies lose energy by direct viscous dissipations as their average size increases, until ultimately undisturbed conditions of flow are restored.

It was pointed out earlier that, as a consequence of the power-law approximations, the length scale λ representative of the smaller, dissipating eddies is proportional to $x^{\frac{1}{2}}$ throughout the flow fields. As evident from table 4, the length scale L representative of the larger, energy-containing eddies in general varies with a power of x smaller than $\frac{1}{2}$. Batchelor & Townsend (1948*a*) have used this fact to explain why the power laws for the development of homogeneous turbulence must change from zone to zone; this explanation can now also be extended to the development of flow past any source of turbulence. As the ratio L/λ, which is proportional to $x^{m'-\frac{1}{2}}$, decreases, the range of eddy sizes present in the flow becomes continuously smaller. Since it is physically impossible for this trend to persist without limit, L/λ is bound to approach a constant value, that is $m' \to \frac{1}{2}$, and the power laws of the remaining length and velocity scales must change accordingly. At the same time, the rate of growth of λ must decrease; in the power-law approach this decrease is taken into account by abrupt changes of $U_0\lambda^2/[\nu(x-x_\lambda)]$ and x_λ from zone to zone.

4.2.4. *A new approach*

The wide acceptance of power laws as mathematical formulations for the variation of flow characteristics past a plane source of turbulence must not obscure the fact that no satisfactory deduction of such laws has yet been put forward. The value of the power laws lies in their mathematical simplicity. Their greatest drawback is that they can only serve as approximations over very limited zones. Moreover, since the zone limits are not specified, agreement between analysis and experiment seems rather arbitrary and of no significance except to the extent that all the measured variations of different flow characteristics agree with the respective analytical predictions simultaneously. The actual variation of the dissipation length λ compares most unfavourably with the predicted proportionality $\lambda^2 \sim x$, as can be seen from figure 16. It appears as a rather forced and

unsatisfactory compromise when the factor of proportionality $U_0\lambda^2/[\nu(x-x_y)]$ and the effective origin $x = x_\lambda$ where $\lambda = 0$ are assumed to change abruptly from zone to zone.

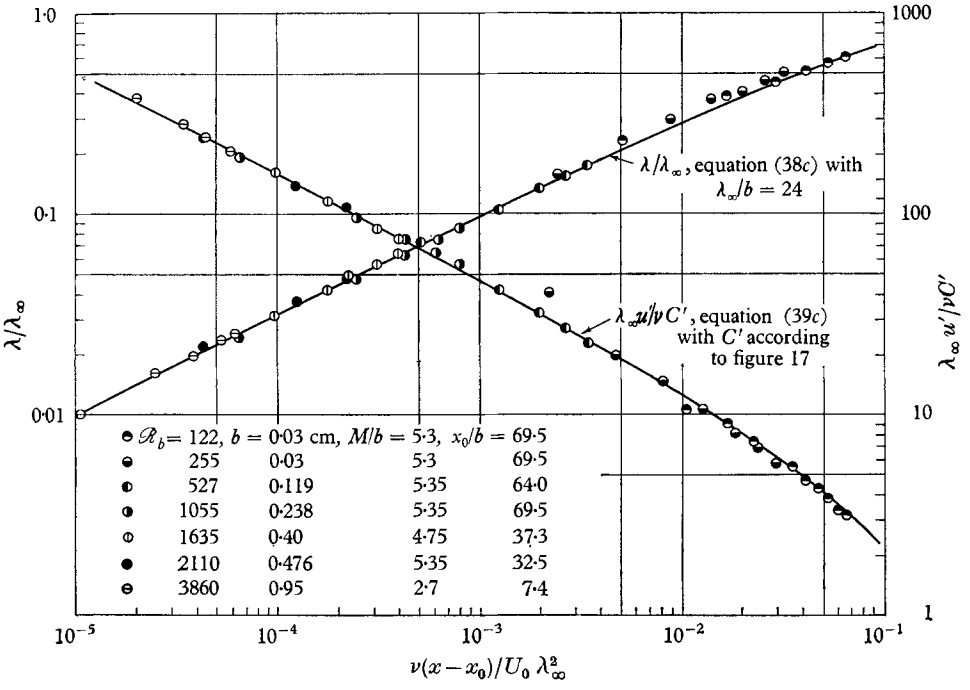

FIGURE 16. Comparison of the trends of equations (38c) and (39c) with corresponding data for grid turbulence. ◓ ◒, Batchelor & Townsend (1948b); ◐ ◑ ●, Batchelor & Townsend (1948a); ⊙ ⊖, Stewart & Townsend (1951).

In the following, an attempt is made to eliminate the arbitrary subdivision of the flow field into limited zones and to replace the discontinuously changing laws of flow development with their undefined range of applicability by regular and overall-applicable functions. There are two ways to approach this objective: by choosing, empirically, a more appropriate formulation of $\lambda(x)$, or by employing more appropriate hypotheses.

The first approach can best be illustrated with the example of a plane source of turbulence. For this case, integration of equation (25) yields directly

$$\frac{u'^2}{U_0^2} = C_u \exp\left(-\frac{10\nu}{U_0}\int\frac{dx}{\lambda^2}\right). \tag{32}$$

If, for the purpose of demonstration, the simple power-law relationship

$$(\lambda/M)^2\mathscr{R}_M = C_\lambda[(x-x_0)/M]^{0.8} \tag{33}$$

is regarded as a sufficiently close approximation for small-enough $\mathscr{R}_\lambda$ (compare figure 16), equation (32) becomes

$$\frac{u'^2}{U_0^2} = C_u \exp\left[-\frac{50}{C_\lambda}\left(\frac{x-x_0}{M}\right)^{0.2}\right]. \tag{34}$$

As evident from figure 12, this equation—with the experimental constants $C_\lambda = 22$ and $C_u = 0{\cdot}0225$ determined by fitting equations (33) and (34) to one pair of data of Batchelor & Townsend (1948*b*)—predicts the actual trend of $u'(x)$ over a considerably wider range of $(x-x_0)/M$ than the $(-\frac{5}{2})$-power and the inverse-square decay law derived by Batchelor & Townsend (1948*c*) and Tan & Ling (1962), respectively.†

The introduction of an empirical relation for $\lambda(x)$ can be avoided by the simultaneous application of two hypotheses:

(*a*) The length scales $r_{\frac{1}{2}}$ (or $y_{\frac{1}{2}}$) and L, representative of the inhomogeneity and the energy-containing eddies, respectively, are proportional to each other, and

(*b*) The correlation function R_r (see figure 11) preserves its shape completely; that is, $L \sim \lambda$.

With the first hypothesis, equation (18) leads to the condition

$$\frac{U_0}{u'_{\max}} \frac{dr_{\frac{1}{2}}}{dx} = \text{const.}, \tag{35}$$

which applies to any flow régime behind either point or line source and is well confirmed by the experiments as evident from table 2.‡ With hypothesis (*b*) added, all length scales involved—namely, $r_{\frac{1}{2}}$ (or $y_{\frac{1}{2}}$), L, and λ—are assumed to vary at equal rates, and equation (18) can be written as

$$u'_{\max}/U_0 = C' \, d\lambda/dx. \tag{36}$$

Like equations (18) and (35), this relation is equally valid for the point and the line source; for the plane source it can be adopted as an approximation to the conditions established by von Kármán & Howarth (1937) for self-preserved correlation functions.§ Substitution of equation (36) into equations (21), (24), and (25) leads to the respective differential equations

$$\left.\begin{aligned} \lambda^2\lambda'' + \lambda\lambda'^2 + \frac{5\nu}{U_0}\lambda' &= 0, \\ \lambda^2\lambda'' + \tfrac{1}{2}\lambda\lambda' + \frac{5\nu}{U_0}\lambda' &= 0, \\ \lambda^2\lambda'' \qquad\quad + \frac{5\nu}{U_0}\lambda' &= 0, \end{aligned}\right\} \tag{37}$$

† The justification for the kinetic model used by Tan & Ling (1962) to deduce the inverse-square law must be questioned, as it would lead to an asymptotic, linear law of growth of the eddy scale, i.e. $\lambda \sim (x-x_0)$, which is contrary to experimental evidence.

‡ When adopted with the power-law approximations, hypothesis (*a*) has the consequences that $2m-n' = 2$ and that the ratio L/λ decreases at an ever-increasing rate rather than tending toward a constant value. Since both of these consequences, particularly the latter, are contrary to experimental observation, hypothesis (*a*) could not be utilized in §4.2.3.

§ Actually, the conditions are $L/\lambda \sim \mathscr{R}_\lambda$ and $u' \sim dL/dx$ in the case of large $\mathscr{R}_\lambda$ when the 'viscous' term in the Kármán–Howarth equation is neglected, and $L/\lambda = \text{const.}$ and $u' \sim \mathscr{R}_\lambda dL/dx$ in the case of small $\mathscr{R}_\lambda$ when the 'convective' term containing the triple-velocity correlation is neglected. In either case, the counterpart of equation (36) for a plane source of turbulence should read $u'/U_0 = C\mathscr{R}_\lambda \, d\lambda/dx$, if $\lambda \, d\mathscr{R}_\lambda/dx$ is ignored in comparison to $\mathscr{R}_\lambda \, d\lambda/dx$ for large $\mathscr{R}_\lambda$. It is remarkable that by replacing $C\mathscr{R}_\lambda$ by a 'constant' C', $\lambda(x)$ and $u'(x)$ are so satisfactorily predicted as shown in figure 16. It seems as though the simplification $C\mathscr{R}_\lambda = C'$ compensates for the fact that the correlation function is not strictly self-preserved.

for a point source, a line source, and a plane source of turbulence, in which primes signify differentiations with respect to x. For a point and a plane source, realistic solutions of these equations are only possible with the limiting conditions $x \to \infty$, $\lambda \to \lambda_\infty$ and $d\lambda/dx \to 0$. By adopting these conditions and the limit $x \to x_0$, $\lambda \to 0$ for all three cases, the solutions become

$$-\frac{5\nu(x-x_0)}{U_0\lambda_\infty^2} = \int_0^{(\lambda/\lambda_\infty)^2} \frac{dz}{\log z} = E + \log\left|\log\left(\frac{\lambda}{\lambda_\infty}\right)^2\right| + \sum_{k=1}^{\infty} \frac{1}{kk!}\left[\log\left(\frac{\lambda}{\lambda_\infty}\right)^2\right]^k, \tag{38a}$$

$$-5\nu(x-x_0)/U_0\lambda_\infty^2 = \log[1-(\lambda/\lambda_\infty)^{\frac{1}{2}}] + \tfrac{1}{3}(\lambda/\lambda_\infty)^{\frac{3}{2}} + \tfrac{1}{2}(\lambda/\lambda_\infty) + (\lambda/\lambda_\infty)^{\frac{1}{2}}, \tag{38b}$$

$$-5\nu(x-x_0)/U_0\lambda_\infty^2 = \log[1-(\lambda/\lambda_\infty)] + \lambda/\lambda_\infty, \tag{38c}$$

and

$$\frac{\lambda_\infty u'_{\max}}{5\nu} = -C' \frac{\log(\lambda/\lambda_\infty)}{\lambda/\lambda_\infty}, \tag{39a}$$

$$\frac{\lambda_\infty u'_{\max}}{5\nu} = -2C' \frac{1-(\lambda/\lambda_\infty)^{\frac{1}{2}}}{\lambda/\lambda_\infty}, \tag{39b}$$

$$\frac{\lambda_\infty u'}{5\nu} = -C' \frac{1-(\lambda/\lambda_\infty)}{\lambda/\lambda_\infty}, \tag{39c}$$

for a point source, a line source, and a plane source of turbulence, respectively; E denotes the Euler constant 0·5772. Corresponding expressions for the variation of $\mathscr{R}_\lambda = \lambda u'_{\max}/\nu$ are obtained from equations (39) through multiplication by $5\lambda/\lambda_\infty$, i.e.

$$\mathscr{R}_\lambda = -5C' \log(\lambda/\lambda_\infty), \tag{40a}$$

$$\mathscr{R}_\lambda = 10C'[1-(\lambda/\lambda_\infty)^{\frac{1}{2}}], \tag{40b}$$

$$\mathscr{R}_\lambda = 5C'[1-(\lambda/\lambda_\infty)]. \tag{40c}$$

The only experimental constants in these equations are λ_∞ and C', the latter evidently being related to the conditions of turbulence generation. As is apparent from equations (40*b*) and (40*c*), respectively, the factors $10C'$ and $5C'$ are identical to the values of $\mathscr{R}_\lambda$ at the virtual origins. As a consequence of the hypothesis that all length scales are proportional to each other, equation (38) describes the variation of any length scale, while equations (39) describe the variation of the only remaining velocity scale in the shear-free régime. A graphical representation of equations (38) and (39) is given in figure 13.

Since the slope of a curve in the logarithmic plot of figure 13 is equivalent to the exponent of a power law, equation (39*b*) is verified by the agreement in the region near the origin between the slope of the velocity curve for a line source and the exponent $-0{\cdot}55$ to $-0{\cdot}6$ for the power law of $u'_{\max}$ evaluated by Townsend (1956) from experiments with a two-dimensional turbulence generator. A verification of equations (38*a*, *c*) and (39*a*, *c*), moreover, is obtained from a comparison with experimental results in figures 14–16, for which purpose values for the axial distance x_0 at which $\lambda = 0$ were adopted from the relevant references. In consideration of the many simplifications and hypotheses that have been necessary to derive these equations, the agreement between analysis and experiment is most remarkable and little depreciated by the fact that the experimental constants were chosen to give the best fit: the constant $\lambda_\infty/D = 0{\cdot}135$ adopted for

a point source of turbulence is of correct order of magnitude according to preliminary measurements of λ; the invariance of λ_∞/b, assumed within the range $100 < \mathscr{R}_b < 4000$ for the plane source of turbulence, appears physically plausible; and the 'constants' C' chosen to fit the data for grid turbulence are uniquely and consistently related to $\mathscr{R}_b$ as shown in figure 17.† The invariance of λ_∞/b can be interpreted as a consequence of two facts: first, the eddies of which λ_∞ is the representative scale are most likely the remains of the largest, originally generated eddies, which are least subject to the cascade process of energy transfer and,

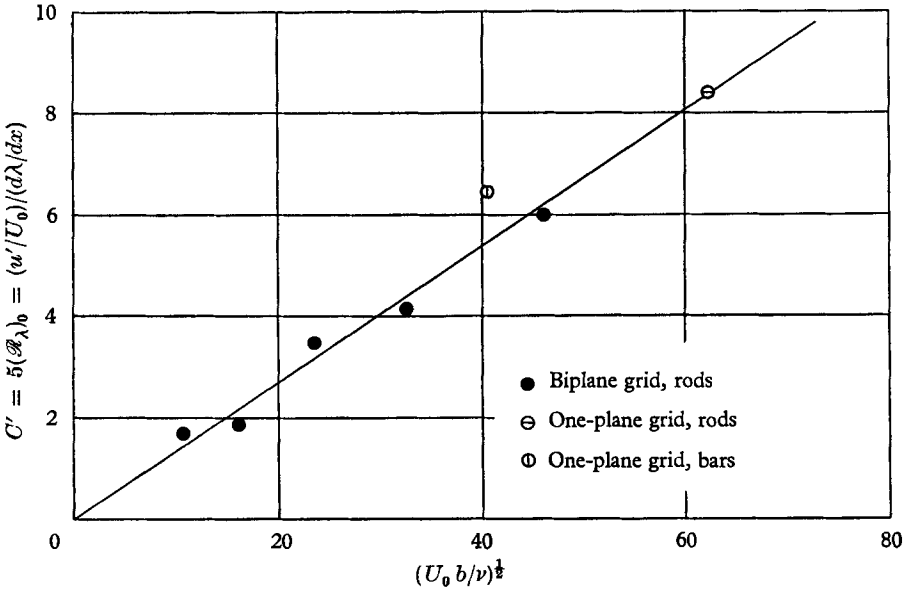

FIGURE 17. Variation of the experimental constant of equation (39*c*) with Reynolds number for grid turbulence according to data. ●, Batchelor & Townsend (1948*a*, *b*); ⊙ ⊖, Stewart & Townsend (1951).

therefore, still proportional in size to a significant length of the turbulence generator, say b;† and, second, since the rate of viscous growth of these eddies increases in the same proportion in which the time of growth diminishes with increasing fluid viscosity, it seems reasonable that viscosity does not affect the magnitude of λ_∞. In other words, the Reynolds-number influence on the growth of λ appears to be completely accounted for in the left-hand term of equation (38), much as the growth of a single vortex filament was found by Rouse & Hsu (1951) to be completely representable in terms of $\nu t/r_0^2$, where r_0 denotes the original vortex size.

† As was first suggested by von Kármán (1938), the rod width b is a more significant length scale for the grid geometry than the mesh width M. Indeed, C' would have shown a less consistent trend if it had been plotted with respect to $\mathscr{R}_M$ instead of $\mathscr{R}_b$. Even more relevant, however, would have been a Reynolds number based on the wake width b_w itself rather than on the width b of the wake generator. The C' value for the grid with rectangular bars would have been in better agreement with the curve in figure 17, and the validity of that curve would have extended to Reynolds numbers outside the range examined, where the ratio b_w/b is expected to change.

Whether λ_∞/D is also an invariant for a point source or a line source of turbulence remains to be investigated. By analogy to the conditions for a plane source discussed, one may speculate that λ_∞/D as well as L_∞/D, $(r_{\frac{1}{2}})_\infty/D$, and $(y_{\frac{1}{2}})_\infty/D$ will depend on the Reynolds number and the body geometry only to the extent that the ratio of the width D_w of the early wake to the body diameter D is affected. The result that the wake width asymptotically approaches a constant value is in itself of great practical interest in regard to wakes of self-propelled bodies and seems to be confirmed by visual observations of condensation trails past jet-propelled aircraft. For the specific Reynolds number and geometry investigated (figure 1), $(r_{\frac{1}{2}})_\infty/D$ is found to be roughly 2·5.

Although equations (38) and (39) are valid only for the shear-free régime, they give a surprisingly good approximation even close to the turbulence generator, as is evident from figures 14 and 15. As λ/λ_∞ becomes very small near the origin, the right-hand sides of equations (38) can be replaced by the terms of lowest power of λ/λ_∞ resulting from a power expansion. Except for the point source of turbulence, the familiar linear variation of λ^2 with $x-x_0$ is thus obtained, the parameter $U_0\lambda^2/[\nu(x-x_0)]$ assuming the values 10, 20, and ∞ for the plane, line, and point source, respectively.† By substituting the relevant value into equation (39*c*), along with the empirical formula

$$(\mathscr{R}_\lambda)_0 = 5C' = 0{\cdot}675\mathscr{R}_b^{\frac{1}{2}} \tag{41}$$

verified in figure 17, the asymptotic law of decay near a plane source of turbulence is obtained in the form

$$u'/U_0 = 0{\cdot}214[(x-x_0)/b]^{-\frac{1}{2}}, \tag{42}$$

which agrees with experimental evidence even so far as the numerical coefficient and the lack of dependence on Reynolds number are concerned (compare also with the commonly accepted power law for the initial zone of decaying homogeneous turbulence).

The Reynolds number $\mathscr{R}_\lambda$, which of all flow characteristics is best suited to define the state of turbulence at any flow section, can now finally be represented as a function of the distance x from the turbulence generator and the conditions $b, \mathscr{R}_b$ of turbulence generation. Upon substitution of equations (38*c*) and (41) and of $\lambda_\infty/b = 24$ in equation (40*c*), one obtains

$$(x-x_0)/b = 115{\cdot}2\mathscr{R}_b[(1{\cdot}48\mathscr{R}_\lambda/\mathscr{R}_b^{\frac{1}{2}}) - 1 - \log(1{\cdot}48\mathscr{R}_\lambda/\mathscr{R}_b^{\frac{1}{2}})] \tag{43}$$

for the plane source of turbulence. This relationship, which is graphically represented in figure 18, is valid at least for grid geometries and Reynolds numbers for which the values of the experimental 'constants' C' and λ_∞/b were verified. For a point source and a line source of turbulence, equivalent relationships can be deduced from equations (40*a*) and (40*b*) when more information with respect to the experimental constants becomes available for these cases.

† According to equations (38), $U_0\lambda^2/[\nu(x-x_0)]$ drops off to zero monotonically as $x \to \infty$. In the case of a plane source, for example, the values 7 and 4, used in the power-law approach to characterize the intermediate and the final zone of decay (table 4), are reached at $\nu(x-x_0)/(U_0\lambda_\infty^2)$ equal, roughly, to 0·027 and 0·16.

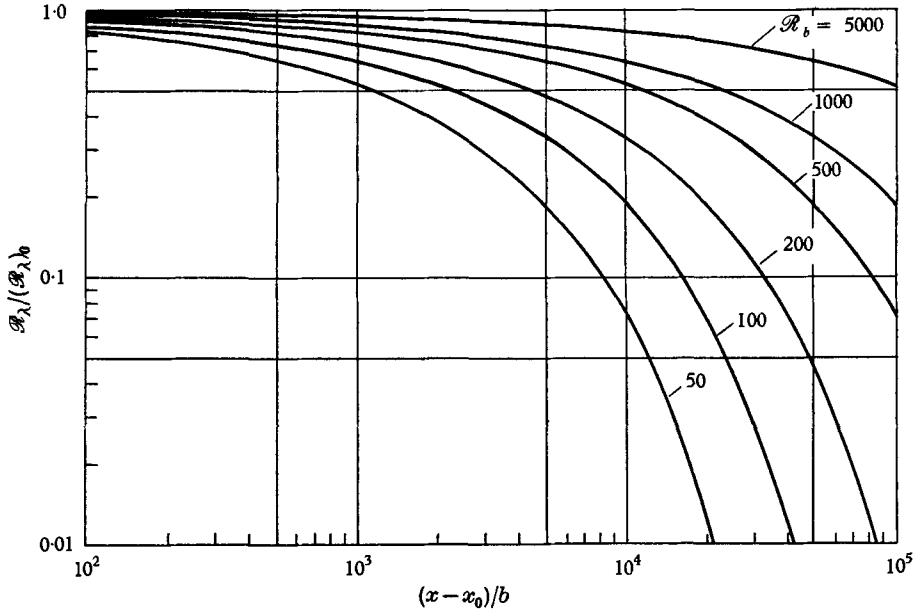

FIGURE 18. Variation of $\mathscr{R}_\lambda$ with axial distance from a plane source of turbulence according to equation (43).

5. Conclusions

Concerned mainly with flow in the wake of an axisymmetric, self-propelled body (i.e. the practical realization of flow past a point source of turbulence) this investigation has revealed significant analogies to elementary free-turbulence shear flows in an initial régime and to decaying homogeneous turbulence in a subsequent shear-free régime. In fact, so far as statistical flow characteristics are concerned, the inhomogeneous turbulence generated by flow past a point source and a line source of turbulence, on the one hand, and the homogeneous turbulence simulated by flow past a plane source like a grid, on the other hand, have proved to be amenable to analogous treatment as axisymmetric, two-dimensional, and one-dimensional counterparts.

As in other free-turbulence flows, the predominant part of the total transfer of energy from the mean to the turbulent motion takes place over an extremely limited zone of pronounced shearing action. Whereas turbulence continues to be produced with distance downstream in elementary free-turbulence shear flows, a practically shear-free régime is rapidly approached behind the various sources of turbulence, and, while the cumulative dissipation rate gradually assumes an axial rate of change equal to that of the cumulative production rate in the former, it tends to approach that of the local convection rate in the latter cases. As in other free-turbulence flows, moreover, the variations of mean-flow and turbulence characteristics in the wake of a self-propelled body exhibit both Reynolds-number similarity and self-preservation. The form of self-preservation, however, is more complex, in that two pairs of velocity and length parameters rather than one are required for its mathematical representation. As a consequence, the

equations of momentum and energy are no longer sufficient for a complete prediction of the axial developments of flow characteristics on a similarity hypothesis alone; they only constitute the necessary relations between these developments—such, for example, as the experimentally confirmed proportionality between the decays of the mean velocity difference and the mean square of the velocity fluctuation.

For the radial variation of turbulence energy in the shear-free régime, a surprisingly good prediction has been found to be the Gaussian error function deduced from the turbulence-energy equation on the additional assumptions of a gradient type of energy diffusion and a phenomenological type of diffusion coefficient. For the axial variation of flow characteristics, power laws have been derived on the hypotheses that changes of the dissipation length with axial distance are identical for respective initial and intermediate zones behind various turbulence sources and that, as experimentally verified, Loitsiansky's parameter remains invariant along the wake centre line. Beside its advantage of mathematical simplicity, this approach permits direct comparison with the well-established approximate theory of decaying homogeneous turbulence; however, not more than the flow development within a vaguely defined and extremely limited intermediate zone and its approximate trend upstream and downstream proved to be predictable thereby.

Substantial improvement over the power-law approach has been achieved through application of the hypothesis that, in the shear-free régime, all length parameters of the flow remain proportional to each other. The axial variation of flow characteristics predicted in this way for flows past a point source, a line source, and a plane source of turbulence agree very closely with corresponding experimental data over the entire range of measurement. Although this agreement may be more indicative of a favourable compensation of inconsistencies involved in the various hypotheses and assumptions than of their relevance, the advantage of the new approach obviously lies in the fact that, with the two experimental constants evaluated, there remains no uncertainty as to the range of axial positions and Reynolds numbers over which the analysis applies. Only with respect to the result that all length parameters approach asymptotically constant values is experimental evidence not quite conclusive; for small Reynolds numbers the turbulent movements cease before the asymptotic range is approached, whereas for large Reynolds numbers this range comes to lie beyond the test section of an ordinary air tunnel.

Results of this study that are worth further investigation are the existence of a more general form of self-preservation than that known from elementary free-turbulence shear flows and the asymptotic axial development of the dissipation length toward a constant value. There is evidence (Naudascher 1964) that the new concept of self-preservation will provide a basis for the analysis of free-shear flows like combined jets and wakes or jets in a general stream, which to date are believed not to be self-preserving. The successful prediction of the dissipation length by a function of x equivalent to a power law with asymptotically decreasing exponent, on the other hand, makes it promising to re-examine such experimental results as the one-fourth-power law obtained by Cooper & Lutzky

(1955) and rejected because of its disagreement with the supposedly well-established one-half-power law of the conventional theory of homogeneous turbulence.

There definitely remains the need to investigate further the physical implications of the hypotheses introduced. Not until the dynamics of the turbulence processes is fully understood and properly reflected in the analysis will the latter be more than a fortunate algebraic approximation to the actual flow development.

The investigation reported here was conducted at the Institute of Hydraulic Research of the University of Iowa under Contract Nonr 1611(03) with the Office of Naval Research, Department of the U.S. Navy. Experimental data were collected by Messrs H. A. Caruso, M. Ridjanovic, and H. Wang. Most of the data reduction and parts of their evaluation were performed by the latter two, both Research Associates of the Institute. Extensive technical assistance with the hot-wire measurements was given by Dr P. G. Hubbard and Mr J. R. Glover. During all phases of the study, valuable clarifications and stimulations were received from discussions with various staff members of the Institute, and the guidance of its director, Dr Hunter Rouse. The manuscript was critically reviewed by Dr Rouse and Dr E. O. Macagno.

REFERENCES

BATCHELOR, G. K. & PROUDMAN, I. 1956 *Phil. Trans. Roy. Soc.* A, **248**, 369.

BATCHELOR, G. K. & STEWART, R. W. 1950 *Quart. J. Mech. & Appl. Maths.* **3**, 1.

BATCHELOR, G. K. & TOWNSEND, A. A. 1948*a* *Proc. Roy. Soc.* A, **193**, 539.

BATCHELOR, G. K. & TOWNSEND, A. A. 1948*b* *Proc. Roy. Soc.* A, **194**, 527.

COOPER, R. D. & LUTZKY, M. 1955 *David Taylor Model Basin Rep.* no. 963.

FRENKIEL, F. N. 1948 *ASME Trans.* **70**, 311.

HUBBARD, P. G. 1957 *Studies in Engng.* University of Iowa, Bulletin 37.

KÁRMÁN, T. von 1938 *Proc. 5th Int. Congr. Appl. Mech.* Cambridge, Mass., p. 347.

KÁRMÁN, T. von & HOWARTH, L. 1938 *Proc. Roy. Soc.* A, **164**, 192.

KOLMOGOROFF, A. N. 1941 *C.R. Acad. Sc. U.R.S.S.* **31**, 538.

LOITSIANSKY, L. G. 1945 *NACA Tech. Memo.* no. 1079.

NAUDASCHER, E. 1964 Discussion of paper no. 64-FE-20 by Curtet, R. & Ricou, F. P. *Trans. ASME, J. Basic Engng*, **86**, no. 4.

RIDJANOVIC, M. 1963 Ph.D. dissertation, University of Iowa.

ROUSE, H. 1960 *La Houille Blanche*, **3** and **4**.

ROUSE, H. & HSU, H. C. 1951 *ASME Proc. First. Nat. Congr. Appl. Mech.* p. 741.

STEWART, R. W. & TOWNSEND, A. A. 1951 *Phil. Trans. Roy. Soc.* A, **243**, 359.

TAN, H. S. & LING, S. C. 1962 Therm Advanced Research. TAR-TR no. 628.

TOWNSEND, A. A. 1949 *Proc. Roy. Soc.* A, **197**, 138.

TOWNSEND, A. A. 1956 *The Structure of Turbulent Shear Flow.* Cambridge University Press.

WANG, H. 1965 Preliminary version of Ph.D. dissertation, University of Iowa.